


Theoretical ground for precursor-based molecular spectroscopyAlexander Makhlin,¹ Panagiotis Papoulias ,² and Eugene Surdutovich^{3,*}¹*Rapid Research, Inc., Southfield, Michigan 48076, USA*²*Science Seals, LLC, Ann Arbor, Michigan 48105, USA*³*Department of Physics, Oakland University, Rochester, Michigan 48309, USA* (Received 26 July 2021; revised 29 September 2021; accepted 30 September 2021; published 22 October 2021)

A theory for excitation of molecular resonances by a train of precursors is developed. Right at the vacuum-medium interface, a train of incident square waves interacts with light electrons and is converted into a train of precursors, which further excite molecular dipoles. Analytic calculations indicate that these excited dipoles generate radiation, including secondary precursors propagating in the backward direction. Encoded in this radiation are proper frequencies of excited molecular dipoles allowing for spectroscopic measurements. The frequency of the train of incident square pulses can be, by several orders of magnitude, smaller than the proper frequencies of molecular resonances.

DOI: [10.1103/PhysRevA.104.042814](https://doi.org/10.1103/PhysRevA.104.042814)**I. INTRODUCTION**

The notion of precursors (the name adopted from seismology) as a physical entity was introduced in optics by Sommerfeld as the solution to an apparent paradox: In the domain of anomalous dispersion, the group velocity can exceed the speed of light c in vacuum. This was obviously in conflict with the special theory of relativity [1,2]. Considering a semi-infinite sinusoidal signal at the interface between vacuum and medium, Sommerfeld proved that the leading part of the signal following the front propagates in the medium with speed c . This leading part is known as a precursor. The physics of this phenomenon was attributed to the dynamic nature of the refraction index $n(\omega)$, which cannot differ from unity until the electronic polarization is engaged in response to electromagnetic wave. In recent years, precursors have attracted attention of both experimentalists and theorists (see, e.g., Refs. [3–13]). An extensive review is given in books by Oughstun [14,15]. In this paper we propose to use precursors for the purpose of spectroscopy.

Traditionally, spectroscopic measurements are conducted in continuous mode and assume the availability of quasi-monochromatic sources of radiation. An underlying assumption is that any properties of measured signals are encoded in the dispersion law of the index of refraction and rely on the availability of high-resolution spectral devices, which may not always be the case, e.g., in millimeter-range radiation. In this paper we propose another approach. Reacting to the steep wave fronts of the incident electromagnetic field, a medium generates, right at the vacuum-medium interface, short pulses, precursors, with their leading fronts traveling through a medium at the speed of light. Precursors are insensitive to any properties of the medium, except for the ubiquitous electronic polarization. However, a long train of primary

precursors can induce and substantially amplify oscillations in molecular dipoles, which subsequently radiate not only in the forward direction, but also in the backward direction with respect to the incident signal.

The present study is founded on the theoretical work [16] by Skrotskaya *et al.* The impetus for their work was provided by advances in the generation of ultrashort optical pulses with steep wave fronts and the possibility of measuring time intervals down to the order of 10^{-14} s.¹ Reference [16] studied the formation of a precursor during traversal of a vacuum-medium interface by the front of a light pulse and its passage through a slab of matter. It was found that precursors can be completely separated from an initial semi-infinite harmonic signal and that, sufficiently close to the leading front, an instantaneous frequency of the precursors' electric field increases with the thickness of the slab, thus making them less and less sensitive to the properties of a medium. Exactly at the leading front, the amplitude of the electromagnetic field remains the same at any distance of its propagation inside the medium and regardless of the number of slabs it crosses. In the present study we build on these physically important facts and suggest that precursors may be utilized in spectroscopic studies of molecules or detection of various chemical substances.

The approach taken in this study is prompted by a large difference of timescales involved in the procedure of measurement and can be briefly described as follows. Let a train of square pulses with sharp wave fronts be incident on a vacuum-medium interface. Light electrons are immediately accelerated and radiate even before they acquire velocity and

¹A successful direct measurement of precursors in a region of anomalous dispersion was reported only by Jeong *et al.* [8]. These measurements triggered an intensive discussion about their interpretation with a focus on the difference between the so-called Sommerfeld and Brillouin precursors [4–7,9].

*Corresponding author: surdutov@oakland.edu

displacement. The electronic component of electric polarization at a time immediately following the wave front can be adequately described by the plasma refraction index $n_e(\omega)$. The scale of this process is determined by the Langmuir frequency $\Omega_e \sim 10^{15}$ – 10^{16} rad/s corresponding to the density of all electrons.² The electric field of precursors produces an external force in the mechanical equations of motion of elastic molecular dipoles; these equations can be solved exactly. The scale of this process is set by the proper frequency $\omega_0 \sim 10^{12}$ rad/s and the width $\Gamma_0 \ll \omega_0$ of a particular molecular resonance. The acceleration of the dipole's constituent charges results in a detectable radiation. The field of this radiation is a sum of slowly varying (with the proper frequency of the elastic dipole's oscillation) electromagnetic fields and of highly oscillating (with the electronic Langmuir frequency) fields of precursors. The proper frequencies of molecular oscillations can be identified by positions of maxima in intensity of backward radiation as functions of duration T of incident pulses (or the frequency $\nu_0 \sim 10^8$ – 10^{10} Hz of the pulses' repetition in the incident train).

The paper is arranged as follows. In Sec. II we consider the first and fastest process of formation of primary precursors at the vacuum-medium interface. We begin with the simplest case of a single step and introduce mathematical methods used throughout the paper. We derive an explicit expression for the electric field of a single precursor and trace its evolution in the course of its propagation inside the medium. Then we consider its passage through an interface and reflection of the incident signal in the form of a single square pulse, which, having both leading and rear fronts, produces two precursors. Finally, we examine propagation of a pulse through a slab of matter with finite thickness.

In Sec. III and Appendix A we solve the equations of motion for elastically bound charges in the field of a train of primary precursors, which originate from an incident train of square pulses. We find an explicit time dependence of the electric dipole moment of the molecule, as well as the ladder of amplitudes of harmonic oscillations that are induced and amplified by the train of precursors. Oscillating dipoles must radiate. Their radiation propagates inside a dispersive medium and eventually escapes into the vacuum. In Sec. IV we find the Green's functions that solve the problem of radiation and also explicitly account for the boundary conditions at the interfaces between the medium and vacuum. We find that dipoles radiate in both the forward and backward directions with respect to the direction of propagation of the train of incident pulses and of the primary precursors.

The expression for the electric field of the molecular dipoles' radiation is derived in Sec. V. The electric dipole polarization induced by the primary precursors includes two distinct components. One of them is proportional to the field of the entire train of primary precursors, which does not lead to radiation and is a strict analytic result. Its presence can be accounted for by small corrections to the purely electronic refraction index. The second component, also found analytically, is due to abrupt jumps in the amplitude of the

elastic dipoles' oscillations. It bears an anticipated harmonic pattern in addition to yet another train of secondary precursors radiated in the backward direction.

In Sec. VIA we analyze and interpret the results obtained in Sec. V. A general discussion and outlook follow in Sec. VIB. Appendixes A–C present some details of analytical calculations in Secs. III and V. In Appendix D a method allowing for numerical calculations elucidating the analytical results obtained in Sec. V and presented in Sec. VIA is shown and discussed.

II. FORMATION AND PROPAGATION OF PRECURSORS

In this section we closely follow Ref. [16], gradually changing the setup of the problem. We start with a semi-infinite incident step pulse propagating from vacuum into a medium and then continue with a single rectangular incident pulse. For the rest of the paper we consider a long train of incident square pulses with alternating polarity. After any wave front crosses an interface, a purely electronic polarization transforms a signal into a precursor.

For a front of a semi-infinite wave incident on a plane interface between the vacuum and a medium, a steady state of propagation is reached after some time has elapsed. The electromagnetic field of a steady state satisfies the extinction theorem of Ewald and Oseen [17,18]; two waves are formed in the medium, a refracted wave with a phase velocity of c/n and a not refracted wave propagating with the speed of light in vacuum. The latter wave exactly cancels out the incident wave in the medium and only a refracted wave is observed. However, a time interval longer than the characteristic time inherent to the medium is required for the steady state to form. During this interval immediately following the wave front (before the refracted and nonrefracted waves are formed), a precursor propagating with the speed of light in the direction of the incident wave is produced.³

Traditionally, an electromagnetic signal in a medium is represented by a sum of harmonics. Each harmonic is a stationary signal, which “knows nothing” of its origin from a limited wave train and behaves as a plane wave in a dispersive medium. Its propagation is described by the stationary index of refraction and stationary boundary conditions, as given by the Fresnel formulas. The electromagnetic characteristics of the medium are determined by natural frequencies ω_q of bound electrons and their relaxation times $\tau_{rel} \sim 1/\Gamma_0$. Within a time interval of about $2\pi/\omega_q$ from the instant of arrival of the wave front at a given point, excitation and relaxation processes play only a secondary role. From the point of view of the damped classical oscillator model, electrons do not have time to acquire either velocity or displacement with respect to their equilibrium positions.

³We caution the reader against thinking that precursors are comprised of the highest harmonics of an incident signal. Harmonics with frequencies, which are above the Langmuir frequency, penetrate a medium and propagate in it. At the same time, the field of precursors is nearly a harmonic signal with the Langmuir frequency (see, e.g., Fig. 2 below).

²This estimate of Langmuir (plasma) frequency, $\Omega_e^2 = 4\pi N_e e^2/m_e$, is of the same order of magnitude for any condensed state.

A. Introductory calculations, an incident step signal

We examine the properties of precursors and consider the propagation of various signals in the simplest case, i.e., when a medium has no molecular resonances, while polarization due to light electrons completely determines the index of refraction $n_e(\omega)$,

$$n_e^2(\omega) = 1 - \frac{\Omega_e^2}{\omega^2}, \quad \Omega_e^2 = \frac{4\pi N_e e^2}{m_e}, \quad (2.1)$$

where Ω_e is the Langmuir (plasma) frequency. Even though in anticipated experiments we expect the incident signal to be a long sequence of alternating square pulses, it is instructive to start with a single step of unit amplitude, which has a well-known spectral representation

$$E_0(t, z) = \theta(t - z/c) = \frac{-1}{2\pi i} \int_{ia-\infty}^{ia+\infty} \frac{d\omega}{\omega} e^{-i\omega(t-z/c)}, \quad (2.2)$$

where $\omega/c = k_0$ is the wave vector of propagation in free space. After the leading wave front crosses the vacuum-medium interface, the amplitudes of Fourier components of a signal acquire the transmission factor $\text{Im}(n_e)$, while the wave vector $k_0 = \omega/c$ changes for $k(\omega) = \omega n_e(\omega)/c$. The electric field of such an incident pulse inside the medium is

$$E'_t(t, z) = \frac{-1}{2\pi i} \int_{ia-\infty}^{ia+\infty} \frac{d\omega}{\omega} \text{Im}[n_e(\omega)] e^{-i\Omega_e[\omega t - \sqrt{\omega^2 - 1}\tilde{z}]} \propto \theta(t - z/c), \quad (2.3)$$

where $\omega n_e(\omega) = \Omega_e \sqrt{\omega^2 - 1}$, $\omega = \omega/\Omega_e$, and $\tilde{z} = z/c$. The Fresnel coefficients of transmission \mathfrak{T} and reflection \mathfrak{R} for partial monochromatic waves (on a plane boundary between medium and vacuum and normal incidence) are well known [17],

$$\begin{aligned} \text{Im}(n_e) &= \frac{2}{1+n_e} = \frac{2\omega}{\omega + \sqrt{\omega^2 - 1}} = \frac{1}{n_e} \mathfrak{T}\left(\frac{1}{n_e}\right), \\ \text{Re}(n_e) &= \frac{1-n_e}{1+n_e} = \frac{\omega - \sqrt{\omega^2 - 1}}{\omega + \sqrt{\omega^2 - 1}} = -\mathfrak{R}\left(\frac{1}{n_e}\right). \end{aligned} \quad (2.4)$$

In the integrals like (2.3) the path L of integration along the real axis of ω can be augmented with a semicircle having an infinite radius C_{inf} in the lower half plane of ω , thus forming a closed clockwise contour C_ω (since $t - z/c > 0$, the integral over C_{inf} is zero). The integrand has two branching points at $\omega = \pm\Omega_e$ ($\omega = \pm 1$) and is double valued. It will become single valued after we cut the complex ω plane along the segment of the real axis between the branching points. Since there are no other singularities, one can take for C_ω any closed path encapsulating the cut (see Fig. 1).

In order to compute this contour integral, we resort to the method originally proposed by Denisov [19] and used in Ref. [16].⁴ A new variable $\zeta = \omega - \sqrt{\omega^2 - 1}$ corresponds to

⁴An indisputable advantage of this method is that in many cases it yields analytic solutions valid throughout all ranges of time t and distance z . Contrary to more popular asymptotic methods of saddle point or steepest descent [1,2,20,21], which provide reasonable approximations only at large times and/or distances, Denisov's

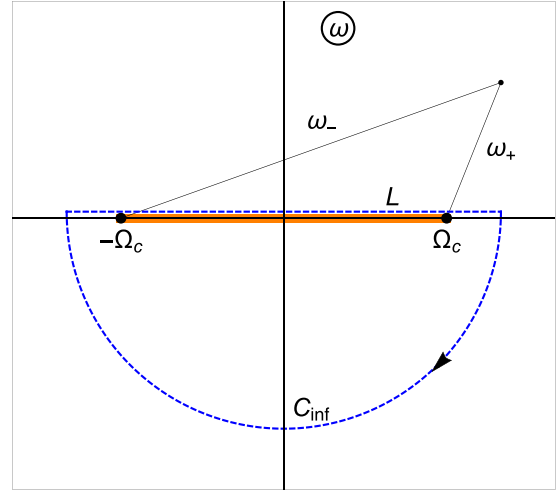


FIG. 1. Cut in the complex ω plane and the integration contour C_ω .

that branch of the conformal mapping $\omega = (\zeta + 1/\zeta)/2$ that maps the complex plane of ω with the cut between branching points $\omega = \pm 1$ onto an exterior of a unit circle $|\zeta| = 1$ in the plane of complex ζ . The integration contour in the ζ plane is a circle with the center at its origin; in all cases considered below, it does not enclose any singularities and it is traversed in the counterclockwise direction. The upper and lower banks of the cut in the ω plane are mapped onto the upper and lower semicircles in the ζ plane, respectively. The phases of complex functions $\omega_+ = \omega - \Omega$ and $\omega_- = \omega + \Omega$ are fixed in such a way that for real $\omega > \Omega_e$, we have $\arg(\omega_+) = \arg(\omega_-) = 0$. Then, for $|\omega| < \Omega_e$, we have $\arg(\omega_+) = \pi$ and $\arg(\omega_-) = 0$ on the upper bank of the cut, with $\text{Re}(k_z) = 0$ and $\text{Im}(k_z) > 0$, as expected.

It is straightforward to check the following formulas, which will often be used throughout the paper:

$$\begin{aligned} \omega &= \frac{1}{2} \left(\frac{1}{\zeta} + \zeta \right), \quad \omega n_e(\omega) = \sqrt{\omega^2 - 1} = \frac{1}{2} \left(\frac{1}{\zeta} - \zeta \right), \\ \frac{d\omega}{\omega} &= -\frac{d\zeta}{\zeta} \frac{1 - \zeta^2}{1 + \zeta^2}, \quad \frac{d\omega}{\omega} \mathfrak{T}[n_e(\omega)] = -\frac{d\zeta}{\zeta} (1 - \zeta^2). \end{aligned} \quad (2.5)$$

The phase factor $e^{-i\Omega_e[\omega t - \sqrt{\omega^2 - 1}\tilde{z}]}$ in the integrand of (2.3) becomes $e^{-i(\Omega_e/2)[(t-\tilde{z})/\zeta + (t+\tilde{z})\zeta]}$ and the integral now reads

$$E'_t(t, z) = \frac{\theta(t - \tilde{z})}{2\pi i} \oint^{(0+)} \frac{d\zeta}{\zeta} (1 - \zeta^2) \times \exp \left\{ -i \frac{\Omega_e \tau}{2} \left[\frac{\xi}{\zeta} + \frac{\zeta}{\xi} \right] \right\}$$

approach works even at the earliest moments of a transient process (which has been reiterated and emphasized in a somewhat different context in Ref. [22]). A theoretical analysis along the traditional guidelines set yet by Sommerfeld and Brillouin (asymptotic calculation of the spectral integrals) has been revisited more than once [4,5,9,23]. In Refs. [14,15] the reader can also find an extensive review of many other papers.

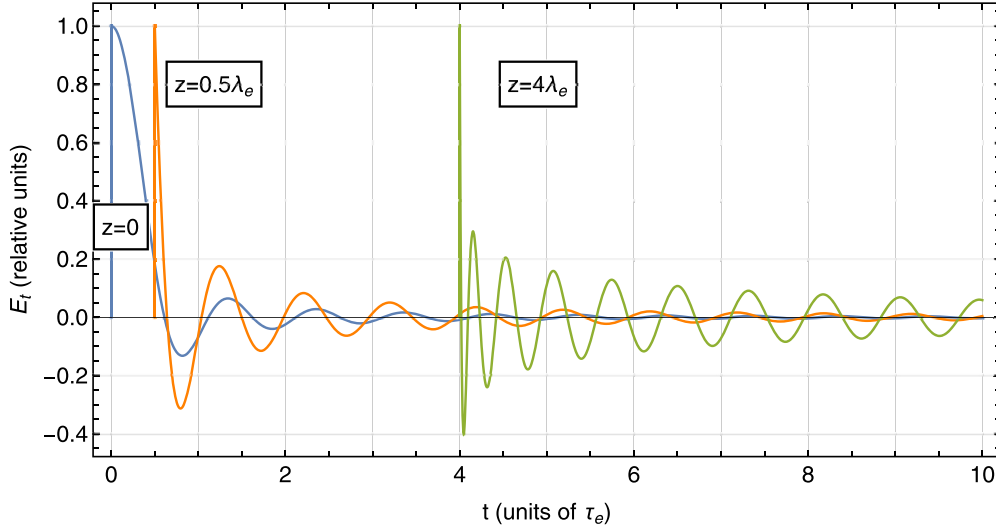


FIG. 2. Plots illustrating the time dependence of precursors formed following a stepwise signal incident on the surface at $z = 0$. Time is measured in periods of plasma oscillations ($\tau_e = 2\pi/\Omega_e$). Time dependences are shown for different depths z (in units of λ_e).

$$= \frac{\theta(t - \tilde{z})}{2\pi i} \oint^{(0+)} \frac{d\xi}{\xi} (1 - \xi^2 \zeta^2) \times \exp \left\{ -i \frac{\Omega_e \tau}{2} \left[\frac{1}{\xi} + \zeta \right] \right\}, \quad (2.6)$$

where $\tau^2 = t^2 - \tilde{z}^2$ and $\xi^2 = (t - \tilde{z})/(t + \tilde{z})$. The factor $\exp\{-iq(\zeta + 1/\zeta)/2\}$ in the integrand of (2.6) is the generating function for the Bessel functions of an integer order⁵

$$\frac{1}{2\pi i} \oint^{(0+)} \frac{d\xi}{\xi^{1+n}} e^{-i(q/2)[\zeta + 1/\zeta]} = (-i)^n J_n(q) = (+i)^n J_{-n}(q). \quad (2.7)$$

The exact analytic answer reads

$$E_t(t, z) \equiv E'_t(t, z) = \theta(t - \tilde{z}) [J_0(\Omega_e \tau) + \xi^2 J_2(\Omega_e \tau)]. \quad (2.8)$$

The results of calculations for Eq. (2.8) are presented in Fig. 2. They are shown as functions of time for different depths z inside a medium.

Several observations reveal the features of precursors that will be important for the rest of our study. First, the deeper the leading front penetrates the medium, the sharper the first maximum is and more rapid the first oscillations are. In other words, in the course of propagation the higher-frequency part of the spectrum of the precursor increases, catching up to the leading front. The Langmuir frequency Ω_e is dominant on a long tail of the precursor and in its full spectrum (see Ref. [16]). Second, regardless of the depth z , the amplitude at the leading front, $ct = z$, stays the same and equal to the amplitude of the incident signal. Third, the drop of the amplitude of plasma oscillations with time at $ct > z$ decreases with increasing depth.

⁵This representation differs from that originally referred to by Denisov [19] [and most often used in the literature, e.g., [24], Sec. 2.2, Eq. (4)], $J_n(q) = \frac{1}{2\pi i} \oint^{(0+)} \frac{dp}{p^{1+n}} e^{(q/2)(p-1/p)} = (-1)^n J_{-n}(q)$, by a trivial change of the variable $\zeta = ip$.

B. Incident single rectangular pulse, reflection, and transmission

Next we consider several examples of interactions between a rectangular incident pulse and a medium. Such a pulse is described as the difference of two step functions shifted in time by T . In the spectral representation, the incident pulse is as follows:

$$E_0(t, z) = \theta(t - z/c) - \theta(t - T - z/c) = \frac{-1}{2\pi i} \int_{ia-\infty}^{ia+\infty} \frac{1 - e^{i\omega T}}{\omega} e^{-i\omega(t-z/c)} d\omega. \quad (2.9)$$

1. Passage and reflection of a pulse at the vacuum-medium interface

Substituting in Eq. (2.3) the spectral density (2.9) of a rectangular pulse yields

$$E_t(t, z) = E'_t(t, z) - E'_t(t - T, z) = \frac{-1}{2\pi i} \int_{ia-\infty}^{ia+\infty} \frac{d\omega}{\omega} \mathfrak{T}[n_e(\omega)] (1 - e^{i\omega T}) e^{-i[\omega t - \omega n_e(\omega) z/c]}, \quad (2.10)$$

where, according to Eq. (2.8), $E'_t(t, z) = \theta(t - \tilde{z}) [J_0(\Omega_e \tau) + \xi^2 J_2(\Omega_e \tau)]$ and, as previously, $\tau^2 = t^2 - \tilde{z}^2$ and $\xi^2 = (t - \tilde{z})/(t + \tilde{z})$. This result is shown in Fig. 3(a) for two different values of z , $z = 0$ and $z = 1.5\lambda_e$. The leading and rear fronts of a rectangular pulse generate precursors of the opposite sign. The evolution of precursors with depth is similar to that observed in Fig. 2.

The spectral form for an electric field of a reflected (back to the vacuum) pulse differs from Eq. (2.3) by replacement of the transmission coefficient \mathfrak{T} with the reflection coefficient \mathfrak{R} and reversing the direction of propagation $z \rightarrow -z$. Then, for the field $E'_r(t, z)$ reflected at the leading front of the incident pulse,

$$E'_r(t, z) = \frac{1}{2\pi i} \int_{ia-\infty}^{ia+\infty} \frac{d\omega}{\omega} \mathfrak{R}(n_e) e^{-i\Omega_e \omega [t+z/c]}. \quad (2.11)$$

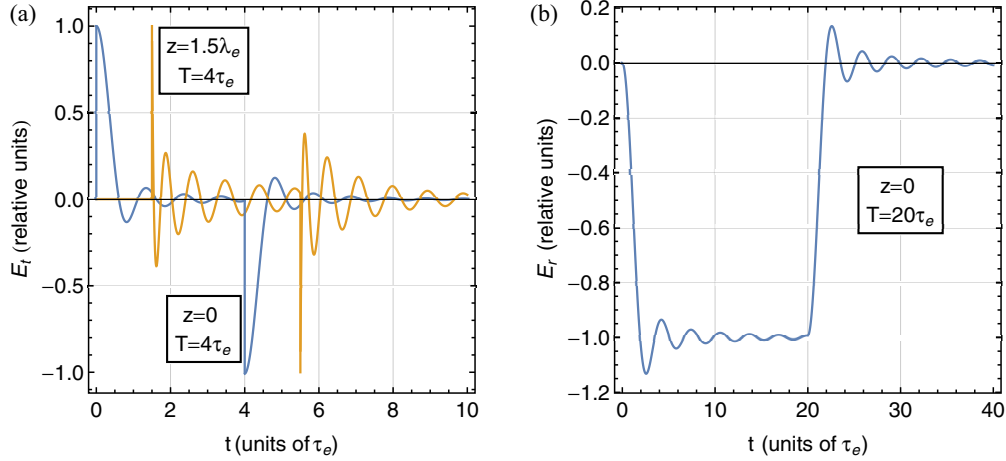


FIG. 3. Two plots illustrating time evolution of precursors produced by a rectangular pulse. (a) Two fronts of an incident rectangular pulse at two depths z . (b) Plot of the reflected pulse in the case of a normal incident wave.

As previously, we resort to (2.5) to rewrite the integrand in terms of the variable ζ . Since $\Re(n_e) = (1 - n_e)/(1 + n_e) = \zeta^2$, we arrive at the following expression for the reflection of a steplike signal:

$$\begin{aligned}
 E_r'(t, z) &= \frac{\theta(t + \tilde{z})}{2\pi i} \oint^{(0+)} \frac{d\zeta}{\zeta} \frac{\zeta^2 - \zeta^4}{1 + \zeta^2} \\
 &\quad \times \exp \left\{ -i \frac{\Omega_e(t + \tilde{z})}{2} \left[\zeta + \frac{1}{\zeta} \right] \right\} \\
 &= \frac{\theta(t + \tilde{z})}{2\pi i} \oint^{(0+)} \frac{d\zeta}{\zeta} \sum_{l=0}^{\infty} (-1)^l [\zeta^{2l+2} - \zeta^{2l+4}] \\
 &\quad \times \exp \left\{ -i \frac{\Omega_e(t + \tilde{z})}{2} \left[\zeta + \frac{1}{\zeta} \right] \right\} \\
 &= -\theta(t + \tilde{z}) \sum_{l=0}^{\infty} \{ J_{2l+2}[\Omega_e(t + \tilde{z})] + J_{2l+4}[\Omega_e(t + \tilde{z})] \} \\
 &= -\theta(t + \tilde{z}) \left\{ 1 - 2 \frac{J_1[\Omega_e(t + \tilde{z})]}{\Omega_e(t + \tilde{z})} \right\}. \quad (2.12)
 \end{aligned}$$

Here the last transformation is based on the identities $1 = J_0(x) + 2J_2(x) + 2J_4(x) + \dots$ and $J_0(x) + J_2(x) = 2J_1(x)/x$ [24]. The exact analytic solution for the reflected field of an incident rectangular pulse is

$$\begin{aligned}
 E_r(t, z) &= E_r'(t, z) - E_r'(t - T, z), \\
 E_r'(t, z) &= \theta(t + \tilde{z}) \left[1 - 2 \frac{J_1[\Omega_e(t + \tilde{z})]}{\Omega_e(t + \tilde{z})} \right]. \quad (2.13)
 \end{aligned}$$

This result is shown in Fig. 3(b). The almost static field of a rectangular pulse cannot propagate in a medium with the refraction index (2.1) and is being reflected. The negative sign of the reflected pulse is due to the boundary condition on the interface $z = 0$, $E_0 + E_r = E_t' \approx 0$, which is self-evident from visual inspection of the two plots in Fig. 3.

2. Transmission of a pulse through a slab

The more realistic problem of passage of a pulse through a slab of thickness d involves two transmission coefficients, one for each interface. For the first interface, as before, the

Fresnel coefficient are $\mathfrak{T}(n)$ and $\mathfrak{T}(1/n)$ for the transmission of the pulse from the slab into the vacuum at $z = d$,

$$E_d'(t, z) = \frac{1}{2\pi i} \int_{ia-\infty}^{ia+\infty} \frac{d\omega}{\omega} \mathfrak{T}(n_e) \mathfrak{T}(1/n_e) e^{-i\omega t + i\omega(z - \tilde{d}) + i\omega n(\omega) \tilde{d}}, \quad (2.14)$$

where $\tilde{z} = z/c$ and $\tilde{d} = d/c$.⁶ By virtue of Eqs. (2.4) and (2.5), in terms of variable ζ , the product $(d\omega/\omega) \mathfrak{T}(n_e) \mathfrak{T}(1/n_e) = 4\sqrt{\omega^2 - 1}(\omega - \sqrt{\omega^2 - 1})d\omega$ becomes $-(d\zeta/\zeta)(\zeta^2 - 1)^2$. Hence, the method outlined in Sec. II A yields

$$\begin{aligned}
 E_d'(t, z) &= \frac{\theta(t - \tilde{z})}{2\pi i} \oint^{(0+)} \frac{d\zeta}{\zeta} (1 - 2\xi^2\zeta^2 + \xi^4\zeta^4) \\
 &\quad \times \exp \left\{ -i \frac{\Omega_e \tau}{2} \left[\frac{1}{\zeta} + \zeta \right] \right\} \\
 &= \theta(t - \tilde{z}) [J_0(\Omega_e \tau) + 2\xi^2 J_2(\Omega_e \tau) + \xi^4 J_4(\Omega_e \tau)], \quad (2.15)
 \end{aligned}$$

where $\tau^2 = (t - \tilde{z})(t - \tilde{z} + 2\tilde{d})$ and $\xi^2 = (t - \tilde{z})/(t - \tilde{z} + 2\tilde{d})$, with $z \geq d$. For a rectangular pulse $E_d(t, z) = E_d'(t, z) - E_d'(t - T, z)$ (see Fig. 4). This is precisely the result obtained in Ref. [16] under the assumption that the harmonic wave experiences total internal reflection on the second boundary of the slab. This can be expected since plasma is optically less dense than vacuum, $n_e(\omega) < 1$, and only the precursor passes through. Also, Fig. 4 clearly indicates that the thicker the slab is, the sharper the leading and rear fronts are of the precursors transmitted through a slab into the vacuum.

III. EXCITATION OF MOLECULAR RESONANCES BY PRIMARY PRECURSORS

In this section we examine the behavior of charges, which form molecular dipoles, in the field of primary precursors. These dipoles become the sources of secondary radiation that carries the desired information about important parameters of dipoles and can be detected. For the sake of simplicity, we

⁶Multiple reflections in the slab are ignored.

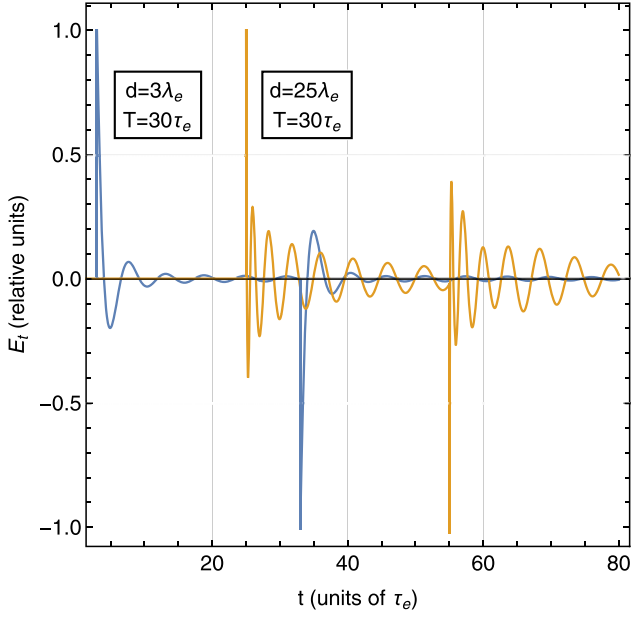


FIG. 4. Plot illustrating the time dependence of precursors that passed through a slab with thicknesses $d = 3\lambda_e$ and $25\lambda_e$. The duration of the incident pulse is $T = 30\tau_e$.

consider only induced dipoles, which is common in molecular optics and is well motivated for transient processes.

Let us consider an elastic molecular dipole in the electric field $E_t(t|z_0)$ of a precursor created at the interface between

vacuum and medium by plasma oscillations of light electrons. Its equation of motion can be written as

$$\ddot{X}(t, z) + 2\Gamma_0\dot{X}(t, z) + \omega_m^2 X(t, z) = \frac{qE_t(t, z)}{M}, \quad (3.1)$$

where M and q are the effective mass and charge of the dipole, X is its displacement, and ω_m and Γ_0 are its proper frequency and width, respectively.

Let a train of square pulses of duration T be incident perpendicularly on the boundary at the point $z = 0$ and time $t = 0$. Equation (2.2) can now be generalized as

$$\begin{aligned} E_0(t, z) &= \mathcal{E}_0[\theta(t - \tilde{z}) - 2\theta(t - T - \tilde{z}) \\ &\quad + 2\theta(t - 2T - \tilde{z}) - \dots] \\ &= \frac{-\mathcal{E}_0}{2\pi i} \int_{-\infty}^{+\infty} \frac{d\omega}{\omega} \sum_{m=1}^{m_p} (-1)^m \epsilon_m e^{im\omega T} e^{-i\omega(t-\tilde{z})}, \end{aligned} \quad (3.2)$$

where ϵ_m is a so-called Neumann symbol ($\epsilon_m = 1$ for $m = 0$ and $\epsilon_m = 2$ for $m \neq 0$) and $m_p = m_p(t)$ is the number of pulses that have passed the boundary $z = 0$ by the time t . A dipole located at z_0 inside the medium is exposed to the electric field,

$$E_t(t, z_0) = \mathcal{E}_0 \sum_{m=0}^{m_p} \epsilon_m (-1)^m \theta(t_* - mT) E'_t(t_* - mT), \quad (3.3)$$

where $t_* = t - \tilde{z}_0 > 0$ and, according to Eqs. (2.3) and (2.8),

$$E'_t(u) = \frac{-\mathcal{E}_0}{2\pi i} \oint_{C_\omega} \frac{d\omega}{\omega} \mathfrak{I}[n_e(\omega)] e^{-i\omega u} e^{-i[\omega - \omega n_e(\omega)]\tilde{z}_0} = \mathcal{E}_0 \theta(u) \left\{ J_0[\Omega_e \sqrt{u(u+2\tilde{z}_0)}] + \frac{u}{u+2\tilde{z}_0} J_2[\Omega_e \sqrt{u(u+2\tilde{z}_0)}] \right\}.$$

For a dipole located at a distance z_0 from the interface between vacuum and the medium, the general solution of Eq. (3.1) reads

$$X(t|z_0) = \frac{q}{M} e^{-\Gamma_0 t} \int_{t_0}^t e^{\Gamma_0 t'} \frac{\sin \omega_0(t-t')}{\omega_0} E_t(t', z_0) dt' + e^{-\Gamma_0 t} [b_c(t_0|z_0) \cos \omega_0 t + b_s(t_0|z_0) \sin \omega_0 t], \quad (3.4)$$

where $\omega_0^2 = \omega_m^2 - \Gamma_0^2$ and constants b_c and b_s are chosen to satisfy the initial conditions at $t = t_0 = z_0/c = \tilde{z}_0$. If this dipole, before being exposed to precursors' field, was at rest, then $X(\tilde{z}_0|z_0) = \dot{X}(\tilde{z}_0|z_0) = 0$ and consequently $b_c = b_s = 0$. Equation (3.4) for this dipole becomes

$$X(t|z_0) = \frac{q}{M} \int_{\tilde{z}_0}^t e^{-\Gamma_0(t-t')} \frac{\sin \omega_0(t-t')}{\omega_0} E_t(t', z_0) dt' = \frac{q}{M} \int_0^{t_*} e^{-\Gamma_0(t_*-t'_*)} \frac{\sin \omega_0(t_*-t'_*)}{\omega_0} E_t(t'_*, z_0) dt'_*, \quad (3.5)$$

where $t_* = t - \tilde{z}_0$ and $t'_* = t' - \tilde{z}_0$.

The source (3.3) in Eqs. (3.1) and (3.5) toggles sign abruptly with each passing pulse and is piecewise continuous. In order for the general solution (3.4) of Eq. (3.1) to be continuous and differentiable throughout the entire time t , we first associate the constants $b_c(t_0)$ and $b_s(t_0)$ with $X_{(m_p)}(m_p T)$ and $\dot{X}_{(m_p)}(m_p T)$ [see Eqs. (A6)]. For the time interval $m_p T < t_* < (m_p + 1)T$ we obtain in (A7) a continuous and differentiable function for every t_* . At the end $(m_p + 1)T$ of this time interval (A7) yields a recursion relation connecting $X_{(m_p)}[(m_p + 1)T] = X_{(m_p+1)}[(m_p + 1)T]$ and $\dot{X}_{(m_p)}[(m_p + 1)T] = \dot{X}_{(m_p+1)}[(m_p + 1)T]$ with $X_{(m_p)}(m_p T)$ and $\dot{X}_{(m_p)}(m_p T)$.

The technical part of the cumbersome calculations for $X(t|z_0)$ and its first time derivative $\dot{X}(t|z_0)$ is described in Appendix A, where we also derive recurrence relations (A8) between the $X_{(m_p)}(m_p|z_0)$ and $\dot{X}_{(m_p)}(m_p|z_0)$ with adjacent numbers m_p . In this way we obtain a ladder of amplitudes $b_c(m_p)$ and $b_s(m_p)$ in Eqs. (3.4) and (5.13) for $m_p T < t < (m_p + 1)T$.

Computation of the radiation of molecular dipoles requires determination of $\ddot{X}(t|z_0)$ of the constituent charges; by virtue of (A7),

$$\begin{aligned} \ddot{X}_{(m_p)}(t|z_0) &= \frac{\mathcal{E}_0 q}{M} \sum_{m=0}^{m_p(t_*)} \epsilon_m (-1)^m \theta(t_* - mT) E'_t(t_* - mT) - \frac{\mathcal{E}_0 q}{M} \sum_{m=0}^{m_p(t_*)} \epsilon_m (-1)^m \omega_0 \\ &\times \int_{mT}^{t_*} e^{-\Gamma_0(t_* - t')} \left[\left(1 - \frac{\Gamma_0^2}{\omega_0^2} \right) \sin[\omega_0(t_* - t')] + 2 \frac{\Gamma_0}{\omega_0} \cos[\omega_0(t_* - t')] \right] \theta(t' - mT) E'_t(t' - mT) dt' \\ &+ \omega_0^2 \left\{ - \left[\left(1 + \frac{\Gamma_0^2}{\omega_0^2} \right) X_{(m_p)}(m_p T) + 2 \frac{\Gamma_0}{\omega_0} \frac{\dot{X}_{(m_p)}(m_p T)}{\omega_0} \right] \cos \omega_0(t_* - m_p T) \right. \\ &\left. + \left[\frac{\Gamma_0}{\omega_0} \left(1 + \frac{\Gamma_0^2}{\omega_0^2} \right) X_{(m_p)}(m_p T) - \left(1 - \frac{\Gamma_0^2}{\omega_0^2} \right) \frac{\dot{X}_{(m_p)}(m_p T)}{\omega_0} \right] \sin \omega_0(t_* - m_p T) \right\} e^{-\Gamma_0(t_* - m_p T)}. \end{aligned} \quad (3.6)$$

The second derivative of the density of the dipole polarization now is $4\pi \ddot{\mathcal{P}}_{\text{mol}}(t) = 4\pi q \langle N_q \ddot{X}(t) \rangle$. We group $\ddot{\mathcal{P}}_{\text{mol}}(t|z_0)$ into the three terms $\ddot{\mathcal{P}}_{\text{mol}}(t|z_0) = \ddot{\mathcal{P}}_a(t|z_0) + \ddot{\mathcal{P}}_b(t|z_0) + \ddot{\mathcal{P}}_c(t|z_0)$,

$$4\pi \ddot{\mathcal{P}}_a(t|z_0) = \Omega_q^2 \mathcal{E}_0 \sum_{m=0}^{m_p(t_*)} \epsilon_m (-1)^m E'_t(t_* - mT), \quad (3.7a)$$

$$\begin{aligned} 4\pi \ddot{\mathcal{P}}_b(t|z_0) &= -\Omega_q^2 \mathcal{E}_0 \sum_{m=0}^{m_p(t_*)} \epsilon_m (-1)^m \omega_0 \int_{mT}^{t_*} e^{-\Gamma_0(t_* - t')} \\ &\times \left[\left(1 - \frac{\Gamma_0^2}{\omega_0^2} \right) \sin[\omega_0(t_* - t')] + 2 \frac{\Gamma_0}{\omega_0} \cos[\omega_0(t_* - t')] \right] E'_t(t' - mT) dt', \end{aligned} \quad (3.7b)$$

$$4\pi \ddot{\mathcal{P}}_c(t|z_0) = 4\pi \Omega_e^2 \omega_0^2 e^{-\Gamma_0(t_* - m_p T)} \{ C_1(m_p T) \cos \omega_0(t_* - m_p T) + C_2(m_p T) \sin \omega_0(t_* - m_p T) \}, \quad (3.7c)$$

where $\Omega_q^2 = 4\pi q^2 N_q / M$ and

$$C_1(m_p T) = - \left[\left(1 + \frac{\Gamma_0^2}{\omega_0^2} \right) \mathcal{P}(m_p T) + 2 \frac{\Gamma_0}{\omega_0} \frac{\dot{\mathcal{P}}(m_p T)}{\omega_0} \right], \quad C_2(m_p T) = \left[\frac{\Gamma_0}{\omega_0} \left(1 + \frac{\Gamma_0^2}{\omega_0^2} \right) \mathcal{P}(m_p T) - \left(1 - \frac{\Gamma_0^2}{\omega_0^2} \right) \frac{\dot{\mathcal{P}}(m_p T)}{\omega_0} \right]. \quad (3.8)$$

For $t_* < T$ (and $m_p = 0$) we have $\mathcal{P}_c(t|z_0) = 0$. The difference between these three parts of \mathcal{P}_{mol} will be discussed in detail when we will be looking at their contributions to the field of the dipole's radiation in Sec. V.

IV. RADIATION EMITTED BY EXCITED MOLECULAR RESONANCES: GENERAL EQUATIONS

The goal of this and the following sections is to find an explicit form for the field of radiation caused by the polarization field derived in the preceding section. We consider the radiation due to uniformly distributed molecular dipoles of number density N_q in an infinitely thin slab of thickness Δz_0 perpendicular to the z axis. The electric field of their radiation $\mathcal{E}_{\text{rad}} = \mathcal{E}$ satisfies the wave equation

$$\frac{\partial^2 \mathcal{E}(t, z)}{\partial z^2} - \frac{1}{c^2} \frac{\partial^2 \mathcal{E}(t, z)}{\partial t^2} = \frac{4\pi}{c^2} [\ddot{\mathcal{P}}_e(t, z) + \ddot{\mathcal{P}}_{\text{mol}}(t, z)], \quad (4.1)$$

where $\mathcal{P}_e(t, z)$ and $\mathcal{P}_{\text{mol}}(t, z)$ are the electronic and molecular components of the electric polarization, respectively. The former, $\ddot{\mathcal{P}}_e(t, z)$, is determined from the equation of motion of free charges,

$$4\pi \ddot{\mathcal{P}}_e(t, z) = 4\pi e N_e \ddot{X}_e(t|z) = 4\pi e N_e \left(\frac{e}{m} \right) \mathcal{E}(t, z) = \Omega_e^2 \mathcal{E}(t, z).$$

The latter, $\ddot{\mathcal{P}}_{\text{mol}}(t, z)$, was computed in Sec. III as the response of molecular dipoles to the field of primary precursors. In the adopted approximation, all effects of the electronic polarization can be incorporated in the refraction index $n_e(\omega)$ so that $\mathcal{P}_e(\omega) = \kappa_e(\omega) \mathcal{E}(\omega)$ and $n_e^2(\omega) = 1 + 4\pi \kappa_e(\omega) = 1 - \Omega_e^2 / \omega^2$. Thus, we are dealing not with the emission of electromagnetic field in vacuum, but rather with the excitation of plasma waves that have well-defined wave fronts and where electrons are involved in a collective process with the electric field. The incident pulses excite these waves producing primary precursors at the interface with vacuum. When they reach and excite molecular resonances in the interior of a medium, the latter must radiate. This radiation propagates in a dispersive medium and it must cross an interface where it exits into the vacuum. As will be shown in Sec. V, by some of its properties this secondary radiation resembles primary precursors.

Let us assume, for the sake of simplicity, that molecular dipoles occupy an infinitely thin layer at depth z_0 so that the source surface density in Eq. (4.1) is $(4\pi/c^2) \ddot{\mathcal{P}}_{\text{mol}}(t, z) = (4\pi/c^2) N_q q \ddot{X}(t|z) \delta(z - z_0) \Delta z_0$. After applying a Fourier transform with

respect to time, Eq. (4.1) reads

$$\frac{\partial^2 \mathcal{E}(v, z|z_0)}{\partial z^2} + \frac{v^2}{c^2} n_e^2(v) \mathcal{E}(v, z|z_0) = \frac{4\pi}{c^2} \ddot{\mathcal{P}}_{\text{mol}}(v, z) \delta(z - z_0) \Delta z_0, \quad (4.2)$$

where the spectral density of molecular polarization

$$\ddot{\mathcal{P}}_{\text{mol}}(v, z) = \int_{-\infty}^{+\infty} \ddot{\mathcal{P}}_{\text{mol}}(t, z) e^{ivt} dt = e^{iv\tilde{z}_0} \int_{-\infty}^{+\infty} \ddot{\mathcal{P}}_{\text{mol}}(t, z) e^{ivt^*} dt^*.$$

In view of the double spectra integrals of the following section, the symbol v is used instead of ω . The solution to Eq. (4.1) can be found via its Green's function $G(\tau, z; t, z_0)$,

$$\mathcal{E}_{\text{rad}}(\tau, z) = \int G(\tau, z; t, z_0) \frac{4\pi}{c^2} \ddot{\mathcal{P}}_{\text{mol}}(t, z_0) dz_0 dt. \quad (4.3)$$

In order to find its explicit expression, let us perform the Fourier transform of Eq. (4.2) with respect to coordinate z . This results in

$$-k^2 \mathcal{E}(v, k|z_0) + \frac{v^2}{c^2} n_e^2(v) \mathcal{E}(v, k|z_0) = \frac{4\pi}{c^2} \ddot{\mathcal{P}}_{\text{mol}}(v, z_0) e^{-ikz_0} \Delta z_0, \quad (4.4)$$

which is an algebraic equation with respect to $\mathcal{E}(v, k|z_0)$. Hence, the electric field inside the medium radiated by molecular dipoles at all depths z_0 can be obtained as the double inverse Fourier transform of (4.4), which then can be integrated over all the radiating dipoles,

$$\mathcal{E}(\tau, z) = \frac{-4\pi}{(2\pi)^2} \int dz_0 \int_{-\infty}^{+\infty} dv \int_{-\infty}^{+\infty} dk \frac{e^{-i[v\tau - k(z-z_0)]}}{c^2 k^2 - v^2 n_e^2(v)} \ddot{\mathcal{P}}_{\text{mol}}(v, z_0). \quad (4.5)$$

We start the calculation of this integral with the integration over k along the real k axis that can be reduced to an integral over a closed contour in the complex k plane ($k = k' + ik''$). The choice of a contour depends on the direction of radiation from the layer of dipoles. Indeed, since $e^{ik(z-z_0)} = e^{ik'(z-z_0)} e^{-k''(z-z_0)}$ for the emission in the forward direction $z > z_0$, we choose to close the contour of integration in the upper half plane, where $k'' > 0$. For the emission backward, $z < z_0$, the contour should be closed in the lower half plane. Technically, these requirements can be implemented by specifying the Green's function in the k plane as $[c^2 k^2 - v^2 + \Omega_e^2 + i\varepsilon_z]^{-1}$, where $i\varepsilon_z$ is an infinitesimal imaginary addition to the wave vector k (compare with Feynman's well-known causal Green's function of QED and also the comprehensive analysis of the radiation principle in a dispersive medium in Ref. [25]). Then the poles corresponding to the propagation in the forward and backward directions lie slightly below and above the real axis, respectively. Performing the k integration by the method of residues in these two cases, we end up with

$$\int_{-\infty}^{+\infty} dk \frac{e^{ik(z-z_0)}}{c^2 k^2 - v^2 n_e^2(v)} = \frac{2\pi i}{2cv n_e(v)} [\theta(z - z_0) e^{ivn_e(v)(z-z_0)/c} + \theta(z_0 - z) e^{-ivn_e(v)(z-z_0)/c}], \quad (4.6)$$

where the first and the second term in square brackets correspond to the emission in the forward and backward directions, respectively. We are interested in the field outside the medium that occupies the slab $0 < z < d$.

To get the field emitted forward, for $z > d$, we must cut off the propagation in the slab at a depth $z = d$, incorporate an additional Fresnel coefficient $\mathfrak{T}[1/n_e(v)]$, and continue propagation for the extra distance $z - d$ in free space. To get the field emitted backward, for $z < 0$, we must account for the in-medium propagation for the distance z_0 , incorporate an additional Fresnel coefficient $\mathfrak{T}[1/n_e(v)]$, and continue propagation for the extra distance, $z < 0$, in free space. The electric field for either direction reads

$$\mathcal{E}(\tau, z > d) = -\frac{i}{c} \int_0^d dz_0 \int_{-\infty}^{+\infty} \frac{dv}{vn_e(v)} e^{-iv\tau} \ddot{\mathcal{P}}_{\text{mol}}(v|z_0) e^{ivn_e(v)(d-z_0)/c} \mathfrak{T}\left(\frac{1}{n_e(v)}\right) e^{iv(z-d)/c}, \quad (4.7a)$$

$$\mathcal{E}(\tau, z < 0) = -\frac{i}{c} \int_0^d dz_0 \int_{-\infty}^{+\infty} \frac{dv}{vn_e(v)} e^{-iv\tau} \ddot{\mathcal{P}}_{\text{mol}}(v|z_0) e^{ivn_e(v)\tilde{z}_0} \mathfrak{T}\left(\frac{1}{n_e(v)}\right) e^{-ivz/c}, \quad (4.7b)$$

where $\mathfrak{T}(1/n_e) = n_e \mathfrak{T}(n_e)$ and the integral over the real axis in the complex v plane can be transformed into an integral over a clockwise contour C_v^- closed by an arc of a large radius in the lower half plane. The path we take to obtain this result accounts for the fact that normal modes of our problem are not plane waves in the infinite medium. They satisfy the boundary conditions at the interfaces $z = 0$ and $z = d$, which violates translation symmetry in the z direction. Furthermore, the radiation of molecular dipoles depends, as does the field of primary precursors, on the depth z_0 of a particular dipole.

If we express $\ddot{\mathcal{P}}(v|z_0)$ in terms of $\ddot{\mathcal{P}}(t|z_0)$, Eqs. (4.7) acquire the form (4.3), where $G(\tau, z; t, z_0)$ are the corresponding retarded Green's functions that propagate radiation of the source, $\ddot{\mathcal{P}}_{\text{mol}}(t|z_0)$, i.e., of the dipoles induced by precursors at (z_0, t) towards

the points of observation (z, τ) on either side of the slab

$$G(\tau, z > d; t, z_0) = -\frac{i}{4\pi} \oint_{C^-} \frac{dv}{v} \mathfrak{I}[n_e(v)] e^{-iv[(\tau-t)-(z-d)/c]} e^{ivn_e(v)(d-z_0)/c}, \quad (4.8a)$$

$$G(\tau, z < 0; t, z_0) = -\frac{i}{4\pi} \oint_{C^-} \frac{dv}{v} \mathfrak{I}[n_e(v)] e^{-iv(\tau-t-|z|/c)} e^{+ivn_e(v)\tilde{z}_0}. \quad (4.8b)$$

Equations (4.8) describe propagation of the radiated electromagnetic field accounting for the boundary conditions on each interface with the vacuum. These expressions are similar to the integrals (2.3) and (2.6). They also set up the upper limits t_{\max} of a subsequent integration over dt in Eq. (4.3). These conditions, $\tau > t + |\tilde{z}| + \tilde{z}_0$ for the emission backward and $\tau > t + \tilde{z} - \tilde{z}_0$ for the dipole radiation forward, mean that there can be no signal until the leading front of the dipole radiation reaches the point (τ, z) of observation. Only the radiation of the dipole that takes place at $t < \tau - |\tilde{z}| - \tilde{z}_0$ can affect the detector at time τ . In both cases the path of integration dv can be closed by a semicircle in the lower half plane. The lower limit $t_{\min}(m) = \tilde{z}_0 + mT$ is the time when the m th pulse hits the dipole. Notably, these Green's functions depend only on the difference $\tau - t$.

Following the scheme of Sec. III, one can compute these integrals by mapping the complex v plane onto the exterior of a unit circle in the complex ζ plane so that $v = (\Omega_e/2)(1/\zeta + \zeta)$ [cf. Eqs. (2.5)]. The result reads

$$G(\tau, z; t, z_0) = \frac{1}{2} \frac{1}{2\pi i} \oint \frac{d\zeta}{\zeta} (1 - \zeta^2) e^{-i(\Omega_e \rho/2)[\mu/\zeta + \zeta/\mu]} = \frac{\theta(\mu\rho)}{2} [J_0(\Omega_e \rho) + \mu^2 J_2(\Omega_e \rho)], \quad (4.9)$$

where $\rho^2 = (\tau - t - |\tilde{z}|)^2 - \tilde{z}_0^2$, $\mu^2 = (\tau - t - |\tilde{z}| - \tilde{z}_0)/(\tau - t - |\tilde{z}| + \tilde{z}_0)$, and $\mu\rho = \tau - t - (|\tilde{z}| + \tilde{z}_0)$ for $G(\tau, z < 0; t, z_0)$, which describes the propagation at the distance $z_0 + |z|$ backward, and $\rho^2 = [(\tau - t) - (z - d)/c]^2 - (d - z_0)^2/c^2$, $\mu^2 = [(\tau - t) - (z - d)/c - (d - z_0)/c]/[(\tau - t) - (z - d)/c + (d - z_0)/c]$, and $\mu\rho = \tau - t - (\tilde{z} - \tilde{z}_0)$ for $G(\tau, z > d; t, z_0)$, which describes the propagation in the forward direction at a distance $z - z_0$.⁷ Ignoring trivial changes of the arguments $\tau \rightarrow \rho$ and $\xi \rightarrow \mu$, the result (4.9) for the Green's function coincides with the expression (2.8) for the field of the precursor that excites a molecular resonance and is plotted in Fig. 2.

V. RADIATION EMITTED BY EXCITED MOLECULAR RESONANCES: THE ELECTRIC FIELD OF RADIATION

The source $\ddot{\mathcal{P}}_{\text{mol}}$ and the field \mathcal{E}_{rad} of its radiation are grouped into the terms $\ddot{\mathcal{P}}_a + \ddot{\mathcal{P}}_b + \ddot{\mathcal{P}}_c$ and $\mathcal{E}_a + \mathcal{E}_b + \mathcal{E}_c$, respectively. The source $\ddot{\mathcal{P}}$ of a single layer of dipoles located at depth z_0 is given by Eqs. (3.7). The Green's function (4.8b) is used.

A. Structureless (singular) term \mathcal{E}_a and regular term \mathcal{E}_b

The terms $\mathcal{E}_a(\tau, z < 0)$ and $\mathcal{E}_b(\tau, z < 0)$ originate from the $\ddot{\mathcal{P}}_a$ and $\ddot{\mathcal{P}}_b$ parts of polarization, respectively. It is shown below that they do not contribute to the total radiation. The singular part $\ddot{\mathcal{P}}_a$ of the source is given by Eq. (3.7a). Using Eq. (4.3) for the backward emitted part $\mathcal{E}_a(\tau, z < 0|z_0)$ of the electric field yields

$$\begin{aligned} \frac{d\mathcal{E}_a(\tau, z < 0)}{d(\Omega_e \tilde{z}_0)} &= \int_{mT + \tilde{z}_0}^{\tau - |\tilde{z}| - \tilde{z}_0} G(\tau, z < 0; t, z_0) 4\pi \ddot{\mathcal{P}}_a(t|z_0) \frac{d(\Omega_e t)}{\Omega_e^2} \\ &= \frac{\Omega_q^2}{\Omega_e^2} \int_{t_{\min}^*(m)}^{t_{\max}^*} \sum_{m=0}^{m_p(t)} (-1)^m \epsilon_m G(\tau, z < 0; t_*, z_0) E_t'(t_* - mT) d(\Omega_e t_*), \end{aligned} \quad (5.1)$$

where $\Omega_q^2 = 4\pi q^2 N_q/M$, and $t_{\min}^* = mT$ and $t_{\max}^* = \tau - |\tilde{z}| - 2\tilde{z}_0$ are the time it takes the incident front to reach the dipole and the time it takes the front of the dipole radiation to reach the point z of observation outside the medium at time τ , respectively. In the same way, by virtue of (3.7b),

$$\begin{aligned} \frac{d\mathcal{E}_b(\tau, z < 0)}{d(\Omega_e \tilde{z}_0)} &= \int_{mT + \tilde{z}_0}^{\tau - |\tilde{z}| - \tilde{z}_0} G(\tau, z < 0; t, z_0) 4\pi \ddot{\mathcal{P}}_b(t|z_0) \frac{d(\Omega_e t)}{\Omega_e^2} = -\frac{\Omega_q^2}{\Omega_e^2} \sum_{m=0}^{m_p(t)} (-1)^m \epsilon_m \int_{t_{\min}^*(m)}^{t_{\max}^*} d(\Omega_e t_*) G(\tau, z < 0; t_*, z_0) \\ &\quad \times \omega_0 \int_{mT}^{t_*} dt' e^{-\Gamma_0(t_* - t')} \left[\left(1 - \frac{\Gamma_0^2}{\omega_0^2} \right) \sin[\omega_0(t_* - t')] + 2 \frac{\Gamma_0}{\omega_0} \cos[\omega_0(t_* - t')] \right] E_t'(t' - mT). \end{aligned} \quad (5.2)$$

⁷For the dipole's radiation inside a slab, the second term in $G(\tau, 0 < z < z_0; t, z_0)$, $\mu^2 J_2(\Omega_e \rho)$, which originates from the transmission coefficient $\mathfrak{I}[1/n_e(v)]$, would be absent.

Here, according to (2.8) and (4.8b),

$$E'_t(t_* - mT) = \frac{-\mathcal{E}_0}{2\pi i} \oint_{C_\omega^-} \frac{d\omega}{\omega} \mathfrak{T}[n_e(\omega)] e^{-i\omega(t_* - mT)} e^{-i[\omega - \omega n_e(\omega)]\tilde{z}_0} = \mathcal{E}_0 [J_0(\Omega_e \tau_m) + \gamma_m^2 J_2(\Omega_e \tau_m)], \quad (5.3)$$

$$G(\tau, z < 0; t_*, z_0) = \frac{-i}{4\pi} \oint_{C_\nu^-} \frac{d\nu}{\nu} \mathfrak{T}[n_e(\nu)] e^{-i\nu(\tau - t_* - |\tilde{z}| - 2\tilde{z}_0)} e^{-i[\nu - \nu n_e(\nu)]\tilde{z}_0} = [J_0(\Omega_e \rho) + \mu^2 J_2(\Omega_e \rho)]/2, \quad (5.4)$$

where $\tau_m^2 = (t_* - mT)(t_* - mT + 2\tilde{z}_0)$, $\gamma_m^2 = (t_* - mT)/(t_* - mT + 2\tilde{z}_0)$, $\rho^2 = (\tau - t_* - |\tilde{z}| - 2\tilde{z}_0)(\tau - t_* - |\tilde{z}|)$, and $\mu^2 = (\tau - t_* - |\tilde{z}| - 2\tilde{z}_0)/(\tau - t_* - |\tilde{z}|)$. It is noteworthy that the incident field (5.3) is in fact the Green's function, which transforms an incident field that hits the interface, into the field (2.8) of the precursor. The Green's function (5.4) differs from the latter only by the replacement $t \rightarrow \tau - t - |\tilde{z}|$; it transforms the field of the dipole radiation into the wave propagating outside medium. Notably, there is no dependence on the parameters ω_0 and Γ_0 of the molecular dipoles.

To compute the integrals (5.1) and (5.2) we use the integral representations (5.3) for $G(\tau, z < 0; t_*, z_0)$ and $E'_t(t_* - mT)$. Splitting the sine and cosine in Eq. (5.2) into two exponents and integrating dt' , we find that

$$e^{i\omega mT - \Gamma_0 t_*} \int_{mT}^{t_*} e^{-i(\omega + i\Gamma_0)t'} e^{\pm i\omega(t_* - t')} dt' = \frac{i}{\omega + i\Gamma_0 \pm \omega_0} [e^{-i\omega(t_* - mT)} - e^{i(\pm\omega_0 + i\Gamma_0)(t_* - mT)}]. \quad (5.5)$$

Treated as functions of the complex variable ω , these functions are regular and have no pole at the points $\omega = \mp\omega_0 - i\Gamma_0$. The second term in square brackets, which comes from the lower limit of the integration, does not depend on ω and the entire exponent in the integral (5.3) over contour C_ω^- is reduced to $e^{-i[\omega - \omega n_e(\omega)]\tilde{z}_0}$. Its contribution to the contour integral is equal to zero. Indeed, after the conformal transformation (2.5), the contour C_ω^- becomes a circle around the origin in the ζ plane, while the exponent becomes a regular function $e^{-i[\omega - \omega n_e(\omega)]\tilde{z}_0} \rightarrow e^{-i\Omega_e \tilde{z}_0 \zeta}$. Conversely, the exponent stemming from the first term introduces the factor $e^{-i\omega(t_* - mT)} \rightarrow e^{-i\Omega_e(t_* - mT)(1/\zeta + \zeta)/2}$, which has an essential singularity at $\zeta = 0$. Assembling the exponents back into the sine and cosine and omitting the ω -independent exponent in square brackets yields

$$e^{i\omega mT - \Gamma_0 t_*} \int_{mT}^{t_*} e^{-i(\omega + i\Gamma_0)t'} \left\{ \begin{array}{l} \cos[\omega_0(t_* - t')] \\ \sin[\omega_0(t_* - t')] \end{array} \right\} dt' = r(\omega) e^{-i\omega(t_* - mT)} \left\{ \begin{array}{l} i\omega - \Gamma_0 \\ -\omega_0 \end{array} \right\}, \quad (5.6)$$

where $r(\omega) = [(\omega + i\Gamma_0)^2 - \omega_0^2]^{-1}$ is the resonance factor. As shown above, residues at its poles in the ω plane are zero.

Using the spectral representation (5.4) for the Green's function, we can cast Eqs. (5.1) and (5.2) into two similar double spectral integrals

$$\begin{aligned} \frac{d\mathcal{E}_a(\tau, z < 0)}{d(\Omega_e \tilde{z}_0)} &= \frac{\Omega_q^2 \mathcal{E}_0}{2\pi i \Omega_e} \sum_{m=0}^{m_p} \epsilon_m (-1)^m \left(\frac{-i}{4\pi} \right) \oint_{C_\nu^-} \frac{d\nu}{\nu} \mathfrak{T}[n_e(\nu)] e^{-i\nu(\tau - |\tilde{z}|)} e^{i[\nu + \nu n_e(\nu)]\tilde{z}_0} \\ &\quad \times \oint_{C_\omega^-} \frac{d\omega}{\omega} \mathfrak{T}[n_e(\omega)] e^{i\omega mT} e^{-i[\omega - \omega n_e(\omega)]\tilde{z}_0} \int_{t_{\min}^*(m)}^{t_{\max}^*} e^{i(v-\omega)t_*} dt_*, \end{aligned} \quad (5.7)$$

$$\begin{aligned} \frac{d\mathcal{E}_b(\tau, z < 0)}{d(\Omega_e \tilde{z}_0)} &= -\frac{\Omega_q^2 \mathcal{E}_0}{2\pi i \Omega_e} \sum_{m=0}^{m_p} \epsilon_m (-1)^m \left(\frac{-i}{4\pi} \right) \oint_{C_\nu^-} \frac{d\nu}{\nu} \mathfrak{T}[n_e(\nu)] e^{-i\nu(\tau - |\tilde{z}|)} e^{i[\nu + \nu n_e(\nu)]\tilde{z}_0} \\ &\quad \times \oint_{C_\omega^-} \frac{d\omega}{\omega} \mathfrak{T}[n_e(\omega)] r(\omega) [2i\Gamma_0 \omega - \omega_m^2] e^{i\omega mT} e^{-i[\omega - \omega n_e(\omega)]\tilde{z}_0} \int_{t_{\min}^*(m)}^{t_{\max}^*} e^{i(v-\omega)t_*} dt_*. \end{aligned} \quad (5.8)$$

The last integral in the above equations is readily found to be

$$\int_{t_{\min}^*(m)}^{t_{\max}^*} e^{i(v-\omega)t_*} dt = \frac{-i}{\nu - \omega} [e^{i(v-\omega)(\tau - |\tilde{z}| - 2\tilde{z}_0)} - e^{i(v-\omega)mT}]. \quad (5.9)$$

Therefore, we can rewrite Eqs. (5.7) and (5.8) as

$$\begin{aligned} \frac{d\mathcal{E}_a(\tau, z < 0)}{d(\Omega_e \tilde{z}_0)} &= \frac{\Omega_q^2 \mathcal{E}_0}{2\pi i \Omega_e} \left(\frac{-i}{4\pi} \right) \oint_{C_\nu^-} \frac{d\nu}{\nu} \mathfrak{T}[n_e(\nu)] e^{-i[\nu - \nu n_e(\nu)]\tilde{z}_0} \oint_{C_\omega^-} \frac{d\omega}{\omega} \mathfrak{T}[n_e(\omega)] e^{-i[\omega - \omega n_e(\omega)]\tilde{z}_0} \\ &\quad \times \sum_{m=0}^{m_p} \epsilon_m (-1)^m \frac{e^{-i\omega(\tau - |\tilde{z}| - 2\tilde{z}_0 - mT)} - e^{-i\nu(\tau - |\tilde{z}| - 2\tilde{z}_0 - mT)}}{\nu - \omega}, \end{aligned} \quad (5.10)$$

$$\begin{aligned} \frac{d\mathcal{E}_b(\tau, z < 0)}{d(\Omega_e \tilde{z}_0)} &= -\frac{\Omega_q^2 \mathcal{E}_0}{2\pi i \Omega_e} \left(\frac{-i}{4\pi} \right) \oint_{C_\nu^-} \frac{d\nu}{\nu} \mathfrak{T}[n_e(\nu)] e^{-i[\nu - \nu n_e(\nu)]\tilde{z}_0} \oint_{C_\omega^-} \frac{d\omega}{\omega} \mathfrak{T}[n_e(\omega)] r(\omega) [2i\Gamma_0 \omega - \omega_m^2] e^{-i[\omega - \omega n_e(\omega)]\tilde{z}_0} \\ &\quad \times \sum_{m=0}^{m_p} \epsilon_m (-1)^m \frac{e^{-i\omega(\tau - |\tilde{z}| - 2\tilde{z}_0 - mT)} - e^{-i\nu(\tau - |\tilde{z}| - 2\tilde{z}_0 - mT)}}{\nu - \omega}. \end{aligned} \quad (5.11)$$

The integrands, as functions of two complex variables ω and ν , have a removable singularity at $\omega = \nu$ in either of the two complex planes and the residue in these poles equals zero. Further analytic calculations, which are described in Appendix C, show that

$$\frac{d\mathcal{E}_a(\tau, z < 0)}{d(\Omega_e \tilde{z}_0)} = \frac{d\mathcal{E}_b(\tau, z < 0)}{d(\Omega_e \tilde{z}_0)} = 0. \quad (5.12)$$

This result could have been anticipated from the viewpoint of the rigorous theory of dispersion [17,18]. Indeed, the terms \mathcal{P}_a and \mathcal{P}_b represent a linear polarization response of the molecular resonances to the external fields of the entire train (3.3) of primary precursors with zero initial conditions $X(\tilde{z}_0|z_0) = \dot{X}(\tilde{z}_0|z_0) = 0$, which are equivalent to Eqs. (A3). The m -dependent limits of integration in Eqs. (5.1) and (5.2) come from the theta functions $\theta(t_* - mT)$ in Eq. (3.3). The absence of backward radiation (scattering) from the components \mathcal{P}_a and \mathcal{P}_b indicates that they satisfy, along with \mathcal{P}_e , the homogeneous wave equation for an average polarization \mathcal{P} with a refraction index $n(\omega)$, which is the main postulate of molecular optics (see Sec. 2.4 of the textbook by Born and Wolf [17] and, especially, Chap. VI of lectures by Rosenfeld [18]).

B. Oscillatory term \mathcal{E}_c

With the $\ddot{\mathcal{P}}_c$ defined by Eq. (3.7c) and the Green's function (4.8b), the component \mathcal{E}_c of the radiation field reads

$$\begin{aligned} \frac{d\mathcal{E}_c(\tau, z < 0|z_0)}{(\Omega_e d\tilde{z}_0)} &= \int G(\tau, z; t, z_0) \Omega_e^{-2} 4\pi \ddot{\mathcal{P}}_c(t|z_0) d(\Omega_e t) = 4\pi \omega_0^2 \int_{t_{\min}(m_p)}^{t_{\max}} d(\Omega_e t_*) e^{-\Gamma_0(t_* - m_p T)} \\ &\times \frac{-i}{4\pi} \oint_{C^-} \frac{d\nu}{\nu} \mathfrak{T}[n_e(\nu)] e^{-i\nu(\tau - t_* - |\tilde{z}|)} e^{+i[\nu + \nu n_e(\nu)]\tilde{z}_0} \{C_1 \cos[\omega_0(t_* - m_p T)] + C_2 \sin[\omega_0(t_* - m_p T)]\}, \end{aligned} \quad (5.13)$$

where coefficients $C_1(m_p T)$ and $C_2(m_p T)$ are defined in Eqs. (3.8) and, according to (A8), all the $\mathcal{P}(m_p T)$ carry the same dimensionless factor Ω_e^2/Ω_e^2 . The final integration dt_* is carried out after the ladder of amplitudes of free oscillations from $m = 0$ to $m = m_p$ is built according to the recursive relations (A7). Taking the Green's function in the form (4.8b), we integrate over t_* between $t_{\min}^* = m_p T$ and $t_{\max}^* = \tau - |\tilde{z}| - 2\tilde{z}_0$,

$$e^{+\Gamma_0 m_p T} \int_{t_{\min}^*}^{t_{\max}^*} e^{i(\nu + i\Gamma_0)t_*} [(C_1 - iC_2)e^{i\omega_0(t_* - m_p T)} + (C_1 + iC_2)e^{-i\omega_0(t_* - m_p T)}] dt_*. \quad (5.14)$$

Assembling the result (C5) of integration into Eq. (5.13), we arrive at

$$\frac{d\mathcal{E}_c(\tau, z < 0|z_0)}{\Omega_e d\tilde{z}_0} = \frac{4\pi \omega_0^2 \Omega_e^2}{4\pi i} \oint_{C^-} \frac{d\nu}{\nu} \mathfrak{T}[n_e(\nu)] r(\nu) e^{-i[\nu - \nu n_e(\nu)]\tilde{z}_0} \{[\dots] - e^{-i\nu\tau_*} [(i\nu - \Gamma_0)C_1(m_p T) - \omega_0 C_2(m_p T)]\}, \quad (5.15)$$

where $r(\nu) = [(\nu + i\Gamma_0)^2 - \omega_0^2]^{-1}$, $\tau_* = t_{\max}^* - t_{\min}^* = \tau - |\tilde{z}| - 2\tilde{z}_0 - m_p T$, and the expression $[\dots]$ in curly brackets [originating from the upper limit of integration in Eq. (5.14)] is a linear combination of products like $C_{1,2} e^{-\Gamma_0 \tau_*} e^{\pm i\omega_0 \tau_*}$. This term does not contain powers of ν higher than one. Here the only ν -dependent exponent is $e^{-i[\nu - \nu n_e(\nu)]\tilde{z}_0}$. Hence,

$$\oint_{C^-} \frac{d\nu}{\nu} \mathfrak{T}[n_e(\nu)] r(\nu) e^{-i[\nu - \nu n_e(\nu)]\tilde{z}_0} \rightarrow \oint^{(0+)} \frac{d\zeta}{\zeta} (1 - \zeta^2) r(\zeta) e^{-i\Omega_e \tilde{z}_0 \zeta} = 0,$$

and this integral turns to zero after integration over the contour (cf. Appendix C). However, the terms associated with the lower limit, where the product of exponents $e^{-i[\nu - \nu n_e(\nu)]\tilde{z}_0} e^{-i\nu(\tau - |\tilde{z}| - 2\tilde{z}_0 - m_p T)}$ has an essential singularity in the ζ plane, must be retained. Therefore,

$$\frac{d\mathcal{E}_c(\tau, z < 0|z_0)}{d(\Omega_e \tilde{z}_0)} = \frac{4\pi \omega_0^2 \Omega_e^2}{4\pi i} \oint_{C^-} \frac{d\nu}{\nu} \mathfrak{T}[n_e(\nu)] r(\nu) e^{-i\nu(\tau - |\tilde{z}| - 2\tilde{z}_0 - m_p T)} e^{-i[\nu - \nu n_e(\nu)]\tilde{z}_0} [\omega_0 a_1(m_p T) - i\nu a_2(m_p T)], \quad (5.16)$$

where

$$a_1(m_p T) = \left(1 + \frac{\Gamma_0^2}{\omega_0^2}\right) \frac{\dot{\mathcal{P}}(m_p T)}{\omega_0}, \quad a_2(m_p T) = \left(1 + \frac{\Gamma_0^2}{\omega_0^2}\right) \mathcal{P}(m_p T) + 2 \frac{\Gamma_0}{\omega_0} \frac{\dot{\mathcal{P}}(m_p T)}{\omega_0}. \quad (5.17)$$

In terms of variable ζ [cf. Eq. (2.5)] and with the resonance factor $r(\zeta)$ given by Eq. (B2), Eq. (5.16) reads

$$\begin{aligned} \frac{d\mathcal{E}_c(\tau, z < 0|z_0)}{d(\Omega_e \tilde{z}_0)} &= \frac{4\pi \omega_0}{2\pi i} \oint^{(0+)} \frac{d\zeta}{\zeta} \exp \left\{ -i \frac{\Omega_e \Lambda}{2} \left[\frac{\Xi}{\zeta} + \frac{\zeta}{\Xi} \right] \right\} \\ &\times \sum_{l=1}^{\infty} \left[\operatorname{Re} \left(\frac{\sin 2l\vartheta}{\sin \vartheta} \right) \zeta^{2l} + i \operatorname{Im} \left(\frac{\sin(2l+1)\vartheta}{\sin \vartheta} \right) \zeta^{2l+1} \right] \left\{ \omega_0 a_1(m_p T) (1 - \zeta^2) - a_2(m_p T) \frac{i}{2} (\zeta^{-1} - \zeta^3) \right\}, \end{aligned} \quad (5.18)$$

where $\Lambda^2 = (\tau - |\tilde{z}| - m_p T - \tilde{z}_0)^2 - \tilde{z}_0^2$ and $\Xi^2 = (\tau - |\tilde{z}| - m_p T - 2\tilde{z}_0)/(\tau - |\tilde{z}| - m_p T)$. Using the integral representation (2.7) of the Bessel coefficients,

$$\frac{d\mathcal{E}_c(\tau, z < 0|z_0)}{d(\Omega_e \tilde{z}_0)} = \frac{\mathcal{E}_0 \Omega_q^2}{\Omega_e^2} \omega_0 \left\{ \omega_0 a_1(m_p T) [s_1(\Lambda, \Xi) + s_3(\Lambda, \Xi)] - \frac{a_2(m_p T)}{2} [s_2(\Lambda, \Xi) + s_4(\Lambda, \Xi)] \right\}, \quad (5.19)$$

where the factor $\mathcal{E}_0 \Omega_q^2 / \Omega_e^2$, which, starting from (A3), is present in every function $4\pi a_j(m_p T)$, is factored out. The functions $s_j(\Lambda, \Xi)$, which are defined by Eqs. (D1), are the sums of products $\sum_l \Xi^{2l} J_{2l}(\Omega_e \Lambda)$. Their behavior critically depends on the distance z_0 to the interface and cannot be comprehended without foregoing analysis of the primary precursors' propagation presented in Sec. II. This is addressed in detail in Sec. VIA and Appendix D.

VI. SPECTROSCOPY WITH PRECURSORS, RESULTS OF CALCULATIONS, AND DISCUSSION

A. Results of calculations

The main results of this study are represented by Eq. (5.19). This equation reflects an explicit dependence of the field radiated in the backward direction on the time interval $\Delta t = \tau - |\tilde{z}| - m_p T$. It takes the m_p th pulse to travel from the interface to a detector located at some distance z from the vacuum-medium interface, where T is the duration of an individual pulse. The field (5.19) substantially depends on the depth z_0 of a dipole's location in a medium. The expression in curly brackets is the sum of two terms, each of which is a product of an m_p -dependent amplitude and the time-dependent signal.

The time dependence of $a_1(m_p T)$ and $a_2(m_p T)$ shown in Fig. 5 initially increases and eventually levels off, forming a shape that resembles a ladder. When $\Gamma_0 \ll \omega_0$ then, according to Eqs. (5.17), the parameters $a_1(m_p T) \propto \dot{\mathcal{P}}(m_p T)$ and $a_2(m_p T) \propto \mathcal{P}(m_p T)$ approximately coincide with deviations of velocity and displacement from their equilibrium values at the moment when the m_p th pulse hits the dipoles. The precise timing of a hit is critical for attaining an amplification of the amplitude of the dipole oscillation. The maximum velocity after a hit is attained when the duration of a pulse is $T = (n + \frac{1}{2})T_0$, which can be clearly seen in Fig. 5 (where $n = 15$). This hit coincides with the dipole passing through its equilibrium position and $\mathcal{P}(m_p T) \approx 0$. The added $\frac{1}{2}$ accounts for the change of polarity of successive pulses. Even a small deviation from the resonant value of T results in a visible

decrease of the amplitude of velocity, proportional to a_1 , and an increase of the coordinate, proportional to a_2 , so that a_1 and a_2 become comparable. Saturation of both amplitudes with growth of m_p is observed for all T . All calculations shown in Fig. 5 are done with $\Omega_e = 10^{15}$ rad/s, $\omega_0 = 10^{12}$ rad/s, $\Gamma_0 = 4 \times 10^9$ rad/s, and $z_0 = 3\lambda_e$. For larger z_0 , the behavior of the ladder amplitudes remains qualitatively the same except that their values decrease by orders of magnitude. This is illustrated in Fig. 6, where a_1 and a_2 are plotted for $z_0 = 3\lambda_e$ and $z_0 = 7\lambda_e$ with such a nonresonant value of T that a_1 and a_2 are comparable.

In the final answer (5.19) for the electric field $\mathcal{E}_c(\tau, z < 0|z_0)$ of radiation, the ladder amplitudes a_1 and a_2 are multiplied by the oscillating source functions $s_1 + s_3$ and $s_2 + s_4$, respectively. The square of this field (proportional to the radiated power), calculated for several values of T , is shown in Fig. 7(a) for a small $z_0 = 3\lambda_e$.

Here $T = 15.50T_0$ is a resonant value of T . The general condition for the resonance $T_{res} = (n + 1/2)T_0$ provides an opportunity to measure ω_0 ; the difference between adjacent resonances in T is equal to $T_0 = 2\pi/\omega_0$. The beginning of each pulse is accompanied by the precursor, shown in Fig. 7(b). The deeper the molecular dipole is located, the smaller the amplitude is of the associated harmonic oscillations and the more pronounced the secondary precursors are of its backward radiation, which is triggered by the sharp fronts of the primary precursors. This can be seen in Figs. 8 and 9, where we plot, with the same parameters, signals $s_1 + s_3$ and $s_2 + s_4$ for shallow, $z_0 = 3\lambda_e$, and deep, $z_0 \geq 7\lambda_e$, dipoles,

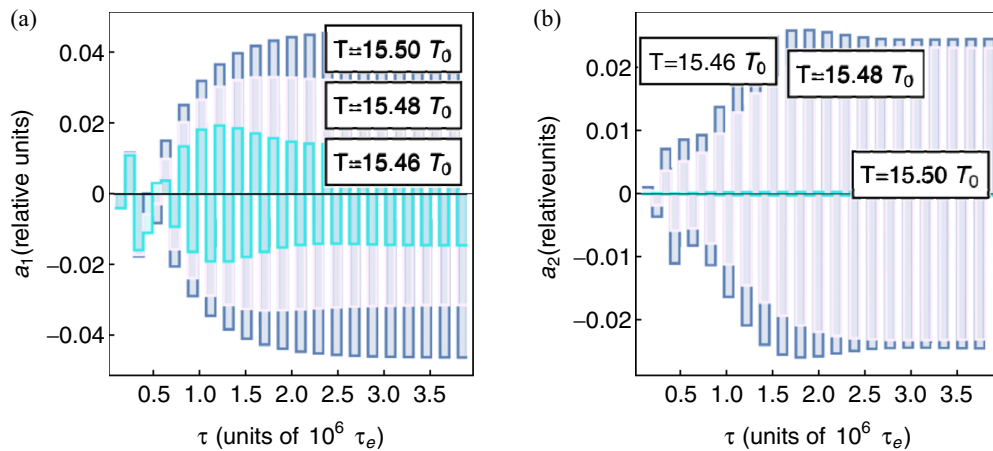


FIG. 5. Time dependence of ladder coefficients (a) a_1 and (b) a_2 . Amplitudes of the ladder parts of the signal level out with time at any value of T . The maxima of combined signals determine the resonant values for T .

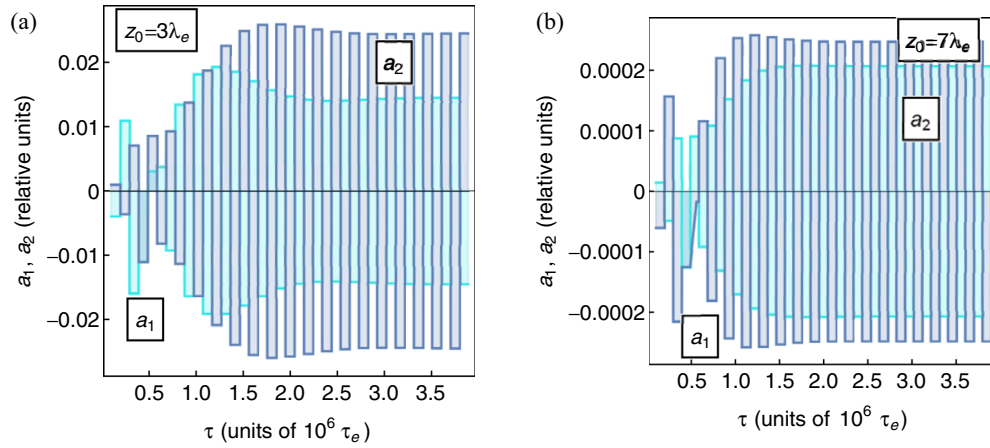


FIG. 6. Comparison of ladder amplitudes for two values of z_0 , (a) $3\lambda_e$ and (b) $7\lambda_e$. The amplitudes of the ladder decrease by the factor of 100 as the depth of the radiating layer increases from $3\lambda_e$ to $7\lambda_e$.

respectively. Every s_j appears to be a sum of a harmonic signal originating from an oscillating dipole and a secondary precursor formed by the electronic polarization near the leading front. The pattern can be qualitatively understood from the dependence of primary precursors on the distance its leading front has penetrated into the medium, as given by Fig. 2. For shallow dipoles, the impulse obtained from the relatively smooth electric field of primary precursors is large and the dipoles immediately begin a harmonic motion, as in Fig. 8. For deeper dipoles, the first peak of the electric field of primary precursors is too sharp to excite harmonic oscillations of large amplitude. Instead, a secondary precursor is produced, as in Fig. 9. This behavior is confirmed by the asymptotic formulas (D15)–(D18), which bear the pattern $J_0(\Omega_e \tau) - \cos(\omega_0 \tau)$, where a molecular harmonic and a precursor are clearly visible.

B. Discussion

Although we intend to measure the same characteristics of matter that are traditionally studied by means of spectroscopy, our approach is quite different. We propose to probe properties of matter by a train of square pulses with sharp wave fronts. This approach does not rely on any kind of spectral device and is motivated by an inherently large difference in scales of the physical processes that result in an actually observed signal and prompt its interpretation. These scales are associated with the Langmuir frequency $\Omega_e \sim 10^{15} - 10^{16}$ rad/s of the electronic component of polarization, the proper frequency $\omega_0 \sim 10^{12}$ rad/s and the width Γ_0 of a molecular resonance, and finally the frequency $\nu_0 \sim 10^8 - 10^{10}$ s $^{-1}$ of the pulses' repetition in the incident train that is used to probe molecular resonances. Each of these processes allows for an exact analytical treatment.

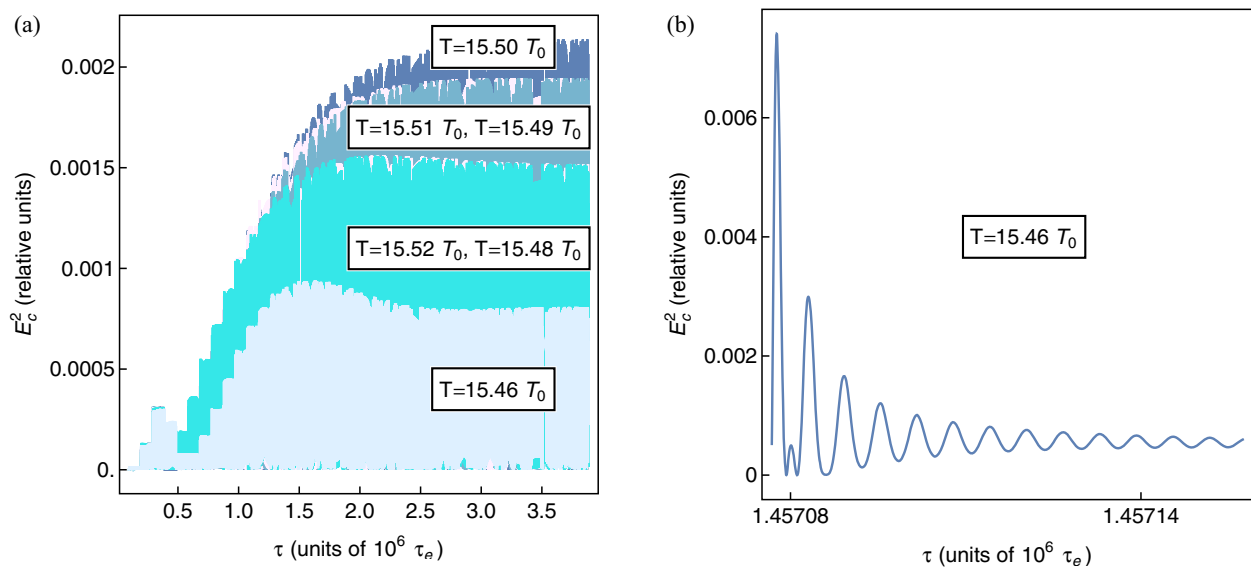


FIG. 7. (a) Square of radiated field from a single layer at $z_0 = 3\lambda_e$ for different values of T in the vicinity of resonant $T = 15.5T_0$. The saturation of amplitude of intensity of the backward radiation is maximized at resonant values of T ; the resonances are rather sharp. Different colors (or shades of gray) show the approach to resonance from $T = 15.46T_0$ to $T = 15.50T_0$ and then a symmetric drop to $T = 15.52T_0$. (b) Each pulse starts with a precursor; an example of such a beginning is shown for $T = 15.46T_0$.

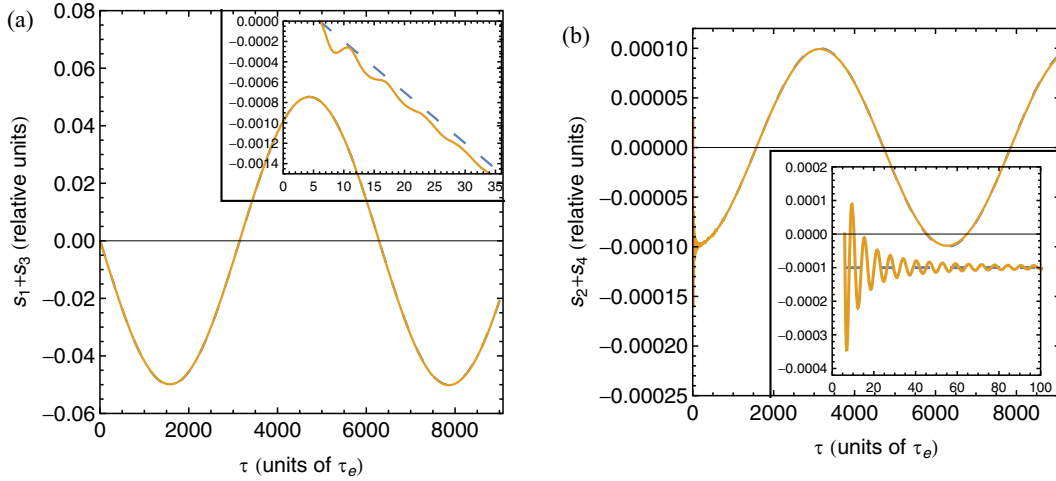


FIG. 8. Time dependence of signals (a) $s_1 + s_3$ and (b) $s_2 + s_4$ for shallow dipoles ($z_0 = 3\lambda_e$). (a) On a large scale the signal (solid line) coincides with a harmonic component (dashed line); on a small scale shown in the inset, the difference due to the precursor is visible at an early time. (b) Same features as in (a), except that in $s_2 + s_4$ the precursor is more pronounced.

The first process is the formation of primary precursors at the vacuum-medium interface. It depends only on the highest frequency Ω_e (2.1), which is translated into the finest time interval $\tau_e = 2\pi/\Omega_e$ and the shortest distance $\lambda_e = c\tau_e$. Its sole parameter is the density of all electrons in a medium. The electric field of primary precursors can be found analytically as light electrons begin to radiate and develop collective behavior forming an index of refraction nearly immediately. Therefore, this stage is totally under the jurisdiction of the rigorous theory of dispersion [17,18]. Our calculations show that in the vicinity of the interface ($z \lesssim 5\lambda_e$), the electric field near the leading front smoothly oscillates. However, the deeper the front penetrates inside a medium, the sharper the first oscillations become. Regardless of how deeply the pulse penetrates a medium, its amplitude at the leading front stays the same as the amplitude of the incident signal.

The second process is the excitation of oscillations in molecular dipoles. The field acting on elastic molecular dipoles is not an incident monochromatic wave or a train of square pulses, but rather a field of precursors formed by the electronic component of polarization. It takes many periods $T_0 = 2\pi/\omega_0$ of proper oscillations to develop a collective behavior of molecular dipoles that would have contributed to the refraction index. In our case this limit is *not* reached. Instead, we address the problem of driving the proper oscillations by a train of primary precursors directly. We solve the equation of motion (3.1) for an elastic molecular dipole, located at a distance z_0 from the interface, in the presence of the electric field (3.3) of the primary precursors. Within the model of a classical oscillator, this problem allows for an analytic solution. We predict that, starting from the first pulses, the amplitudes of the dipole's oscillation would form an ascending ladder that eventually reaches some saturation

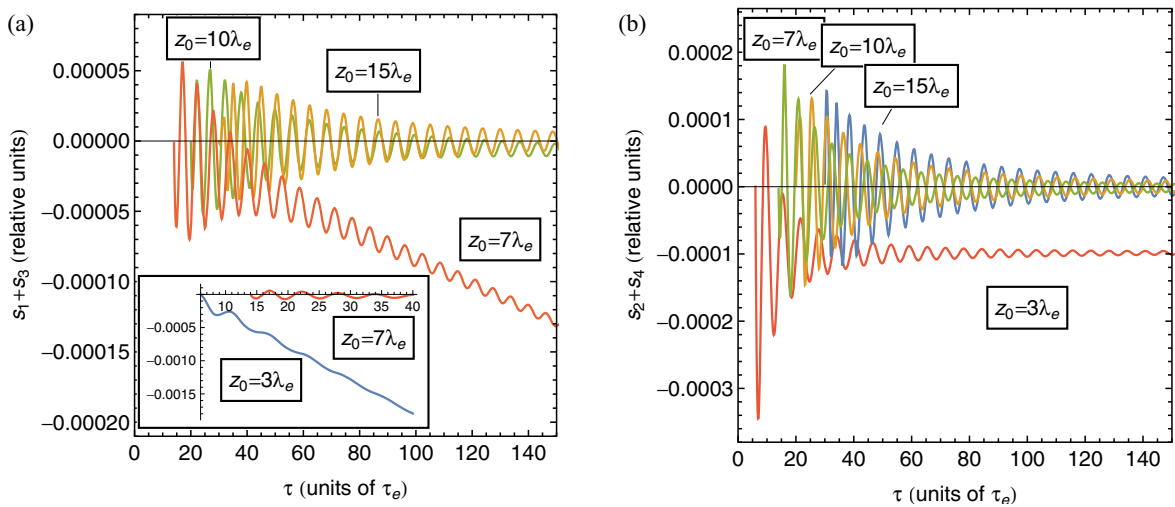


FIG. 9. Comparison of time dependences of signals (a) $s_1 + s_3$ and (b) $s_2 + s_4$ for different values of z_0 . Each signal is a sum of a harmonic signal [(a) negative sine and (b) negative cosine] and an oscillating precursor. As the depth increases, the amplitudes of harmonic parts sharply decrease and the precursor parts (starting from the same amplitude) attenuate less and less.

level, unless the damping $\Gamma_0 = 0$. The former must be maximum when the duration $T = 1/\nu$ of an individual incident pulse is $T_n = (n + \frac{1}{2})T_0 = 2\pi(n + \frac{1}{2})/\omega_0$, which indicates the existence of a resonance. The time interval T_0 between two neighboring resonances determines the frequency of proper oscillations ω_0 .

The third process is the emission of secondary radiation by the oscillating molecular dipoles. We have shown that, in the final answer for the measured signal, the ladder amplitudes are multiplied by the time-dependent source functions, which explicitly depend on time and the distance of a radiating dipole from the interface z_0 . Numerical analysis confirms these functions to be the sums of two distinctive parts. The first part is a harmonic function oscillating with the proper frequency ω_0 of a molecular resonance. It dominates for the dipoles located close to the interface, $z_0 \lesssim 10\lambda_e$, and is due to the oscillations excited by the leading and relatively smooth parts of primary precursors. The second part of the radiated field oscillates with the Langmuir frequency Ω_e and represents the train of secondary precursors, which propagate not only forward, but also in the backward direction with respect to the incident train. Secondary precursors come predominantly from deeply located dipoles, where the near-front oscillations of primary precursors are very fast. This could have been anticipated from a qualitative inspection of Fig. 2.

All numerical calculations were performed with the Wolfram's *Mathematica* software on a standard PC. Because the Lommel's functions are composed of highly oscillating Bessel functions, their numerical implementation meets difficulties. To work around them, we developed a special procedure, which is explained in Appendix D. More accurate calculations may require faster computers.

C. Imagining an experiment

Finally, we would like to discuss the prospect of building a device implementing the proposed idea of precursor-based spectroscopy. Before analyzing the feasibility of this implementation, we discuss one detail related to the theoretical study presented above. It has been shown that dipoles in the medium can be excited by a train of primary precursors formed in response, by the medium, to a train of square pulses. The choice of such a signal has been quite convenient for theoretical analysis; however, it does not provide a smooth transition to choosing a generator for desired experiments. Since ideal square pulses do not exist, the question is about acceptable or desirable generators for the incident signal.

First, an ideal square pulse is not necessary. The propagation of the leading front in a dispersive medium is always accompanied by a precursor, even if the leading front is not steplike [16].⁸ Recall the feature emphasized in Fig. 2, that in

⁸If an incident pulse begins with a linearly growing field, e.g., $E_0(t, z) = \mathcal{E}_0\theta(t - \tilde{z})e^{-(t-\tilde{z})/a} \sinh[(t - \tilde{z})/a]$, then the leading terms of the precursor inside a medium with the Langmuir frequency Ω_e read $E'_l(t, z) = 2\mathcal{E}_0(a\Omega_e)^{-1}\theta(t - \tilde{z})[\xi J_0(\Omega_e\tau) + \xi^3 J_3(\Omega_e\tau) + \dots]$, where, as previously, $\tau^2 = t^2 - \tilde{z}^2$, $\xi^2 = (t - \tilde{z})/(t + \tilde{z})$, $\tilde{z} = z/c$, and the series of omitted terms begins with $\xi^5 J_5(\Omega_e\tau)$. Modulo the factor $(a\Omega_e)^{-1}$, these first two terms reproduce the result obtained

the process of propagation precursors become progressively steeper, decreasing the time interval between their nodes and effectively increasing their frequencies. Thus, even if the highest harmonic of the incident signal is much lower than Ω_e , the harmonics of the precursor will asymptotically approach Ω_e after passing a sufficient length in this medium. Therefore, in order to excite, e.g., a 6-THz line in liquid water, a square pulse generator with a frequency of 6 GHz (allowing sweeping through a range of frequencies in the gigahertz range) should be well suited; such generators are available.

Second, both the amplitude \mathcal{E}_0 and steepness $d\mathcal{E}_0(t, z)/dt$ of the square pulse can be substantially increased by adding a nonlinear transmission line [26,27], which converts even relatively smooth leading fronts of incident pulses into shock waves with widths of approximately or less than 1 ps, at the output of a generator. This will eventually result in an increased amplitude and sharpness of precursors.

Detecting a resonance excited by the train of precursors can be accomplished by endowing the impulse generator with an antenna that emits primary pulse and receives a response signal; the latter serves as a trigger for the next pulse. This scheme (which has been routinely used in radar systems at various frequency ranges since the 1940s) can be used to synchronize the incident signal with the returned signal. It is likely that this will produce a standing wave between the generator and the medium. This intriguing possibility exists due to the secondary precursors emitted in the backward radiation. The harmonic part of the backward radiation with frequency of about a few terahertz can be rectified, e.g., using a Schottky diode as a power detector and measured with a reasonable precision. Considered as a function of the period T (see Fig. 7), this measurement can yield the shape of a resonance curve.

Thus, the accomplishment of the proposed project for precursor spectroscopy seems realistic. We view a conceptual simplicity of the proposed arrangement as an advantage compared to known spectroscopic techniques. Unlike, e.g., the dual comb spectroscopy, which requires a sophisticated optical system, precursor spectroscopy relies on a single impulse generator with a controlled variable frequency in the gigahertz region and a positive feedback that allows for detecting and studying resonances.

ACKNOWLEDGMENTS

The authors are grateful to the anonymous referees for their questions, insightful remarks, and suggestions.

APPENDIX A: CALCULATION OF THE LADDER OF EXCITATIONS

Let $m_p = m_p(t_*)$ be the number of wave fronts that have crossed z_0 by the time t , $m_p T \leq t < (m_p + 1)T$, so that $m_p = 0$ corresponds to the leading front that enters a yet not polarized medium. When the dipole is hit by the next pulse,

in Ref. [16] under the assumption that the semi-infinite harmonic wave $E_0(t, z) = \mathcal{E}_0\theta(t - \tilde{z})\sin[\Omega_e(t - \tilde{z})]$ (where $a\Omega_e = 1$) experiences total internal reflection.

the upper limit $m_p(t_*)$ increases by one. In order to compute $X(t|z_0)$, we substitute (3.3) into Eq. (3.5), which yields

$$X(t|z_0) = \frac{\mathcal{E}_0 q}{M} \int_0^{t_*} K(t_* - t'_*) \left[\sum_{m=0}^{m_p(t_*)} \epsilon_m (-1)^m \theta(t'_* - mT) E'_t(t'_* - mT) \right] dt'_*, \quad (\text{A1})$$

where the kernel $K(t - t')$, the fundamental solution of the differential equation (3.1), and its first two time derivatives are

$$\begin{aligned} K(x) &= \theta(x) e^{-\Gamma_0 x} \frac{\sin \omega_0 x}{\omega_0}, \quad \dot{K}(x) = \frac{dK(x)}{dx} = \theta(x) e^{-\Gamma_0 x} \left[\cos \omega_0 x - \Gamma_0 \frac{\sin \omega_0 x}{\omega_0} \right], \\ \ddot{K}(x) &= \frac{d^2 K(x)}{dx^2} = \delta(x) + \theta(x) e^{-\Gamma_0 x} \left[-2\Gamma_0 \cos \omega_0 x - (\omega_0^2 - \Gamma_0^2) \frac{\sin \omega_0 x}{\omega_0} \right], \quad K(0) = 0, \quad \dot{K}(0) = 1. \end{aligned} \quad (\text{A2})$$

Since we assume that the dipole's charges are initially at rest, then for $0 < t_* < T$,

$$X_{(0)}(t_*) = \frac{\mathcal{E}_0 q}{M} \int_0^{t_*} K(t_* - t') E'_t(t') dt', \quad \dot{X}_{(0)}(t_*) = \frac{\mathcal{E}_0 q}{M} \int_0^{t_*} \dot{K}(t_* - t') E'_t(t') dt', \quad X_{(0)}(0) = \dot{X}_{(0)}(0) = 0. \quad (\text{A3})$$

If the m_p th pulse is passing through a dipole, then for $m_p T < t_* < (m_p + 1)T$,

$$\begin{aligned} X_{(m_p)}(t_*) &= \frac{\mathcal{E}_0 q}{M} \int_{m_p T}^{t_*} K(t_* - t') \left[\sum_{m=0}^{m_p(t_*)} (-1)^m \epsilon_m \theta(t'_* - mT) E'_t(t'_* - mT) \right] dt' \\ &\quad + e^{-\Gamma_0 t_*} [b_c(m_p T) \cos \omega_0 t_* + b_s(m_p T) \sin \omega_0 t_*], \\ \dot{X}_{(m_p)}(t_*) &= \frac{\mathcal{E}_0 q}{M} \int_{m_p T}^{t_*} \dot{K}(t_* - t') \left[\sum_{m=0}^{m_p(t_*)} (-1)^m \epsilon_m \theta(t'_* - mT) E'_t(t'_* - mT) \right] dt' \\ &\quad + e^{-\Gamma_0 t_*} \{ [\omega_0 b_s(m_p T) - \Gamma_0 b_c(m_p T)] \cos \omega_0 t_* - [\omega_0 b_c(m_p T) + \Gamma_0 b_s(m_p T)] \sin \omega_0 t_* \}. \end{aligned} \quad (\text{A4})$$

The coefficients $b_c(m_p T)$ and $b_s(m_p T)$ can be expressed in terms of the dipole's amplitude $X(m_p T)$ and its time derivative $\dot{X}(m_p T)$. The coordinate and velocity at time T are continuous, i.e., their values at the end of the first pulse, $m_p = 0$, and at the beginning of the second pulse, $m_p = 1$, are equal. According to (A3), these are

$$X_{(0)}(T) = X_{(1)}(T) = \frac{\mathcal{E}_0 q}{M} \int_0^T K(T - t') E'_t(t') dt', \quad \dot{X}_{(0)}(T) = \dot{X}_{(1)}(T) = \frac{\mathcal{E}_0 q}{M} \int_0^T \dot{K}(T - t') E'_t(t') dt'.$$

Similarly, if in Eq. (A4) $t_* = m_p T$, at the beginning of the m_p th interval, the integrals become zero and

$$\begin{aligned} X_{(m_p)}(m_p T) &= e^{-\Gamma_0 m_p T} [b_c(m_p T) \cos \omega_0 m_p T + b_s(m_p T) \sin \omega_0 m_p T], \\ \dot{X}_{(m_p)}(m_p T) &= e^{-\Gamma_0 m_p T} \{ [\omega_0 b_s(m_p T) - \Gamma_0 b_c(m_p T)] \cos \omega_0 m_p T - [\omega_0 b_c(m_p T) + \Gamma_0 b_s(m_p T)] \sin \omega_0 m_p T \}. \end{aligned} \quad (\text{A5})$$

Now we can trade $b_c(mT)$ and $b_s(mT)$ for $X(mT)$ and $\dot{X}(mT)$:

$$\begin{aligned} \omega_0 e^{-\Gamma_0 m_p T} b_c(m_p T) &= (\omega_0 \cos \omega_0 m_p T - \Gamma_0 \sin \omega_0 m_p T) X_{(m_p)}(m_p T) - \sin \omega_0 m_p T \dot{X}_{(m_p)}(m_p T), \\ \omega_0 e^{-\Gamma_0 m_p T} b_s(m_p T) &= (\omega_0 \sin \omega_0 m_p T + \Gamma_0 \cos \omega_0 m_p T) X_{(m_p)}(m_p T) + \cos \omega_0 m_p T \dot{X}_{(m_p)}(m_p T). \end{aligned} \quad (\text{A6})$$

Then for $m_p(t_*)T < t_* < [m_p(t_*) + 1]T$,

$$\begin{aligned} X_{(m_p)}(t_*) &= \frac{\mathcal{E}_0 q}{M} \int_{m_p T}^{t_*} K(t_* - t') \sum_{m=0}^{m_p(t_*)} (-1)^m \epsilon_m \theta(t'_* - mT) E'_t(t'_* - mT) dt' \\ &\quad + e^{-\Gamma_0(t_* - m_p T)} \left\{ \left[\cos \omega_0(t_* - m_p T) + \frac{\Gamma_0}{\omega_0} \sin \omega_0(t_* - m_p T) \right] X_{(m_p)}(m_p T) + \sin \omega_0(t_* - m_p T) \frac{\dot{X}_{(m_p)}(m_p T)}{\omega_0} \right\}, \\ \frac{\dot{X}_{(m_p)}(t_*)}{\omega_0} &= \frac{\mathcal{E}_0 q}{M} \int_{m_p T}^{t_*} \frac{\dot{K}(t_* - t')}{\omega_0} \left[\sum_{m=0}^{m_p(t_*)} (-1)^m \epsilon_m \theta(t'_* - mT) E'_t(t'_* - mT) \right] dt' + e^{-\Gamma_0(t_* - m_p T)} \\ &\quad \times \left\{ - \left(1 + \frac{\Gamma_0^2}{\omega_0^2} \right) \sin \omega_0(t_* - m_p T) X_{(m_p)}(m_p T) + \left[\cos \omega_0(t_* - m_p T) - \frac{\Gamma_0}{\omega_0} \sin \omega_0(t_* - m_p T) \right] \frac{\dot{X}_{(m_p)}(m_p T)}{\omega_0} \right\}. \end{aligned} \quad (\text{A7})$$

For $t_* = m_p T$, the above equations become identities. For $t_* = (m_p + 1)T$ in Eqs. (A7), we obtain the recursion formula for coefficients $X_{(m_p)}(m_p T)$, which form the ladder of amplitudes of harmonic oscillations,

$$\begin{aligned} X_{(m_p)}[(m_p + 1)T] &= \frac{\mathcal{E}_0 q}{M} \int_{m_p T}^{(m_p+1)T} K[(m_p + 1)T - t_*] \sum_{m=0}^{m_p(t_*)} (-1)^m \epsilon_m \theta(t_* - mT) E'_t(t_* - mT) dt_* \\ &\quad + e^{-\Gamma_0 T} \left\{ \left[\cos \omega_0 T + \frac{\Gamma_0}{\omega_0} \sin \omega_0 T \right] X_{(m_p)}(m_p T) + \sin \omega_0 T \frac{\dot{X}_{(m_p)}(m_p T)}{\omega_0} \right\}, \\ \frac{\dot{X}_{(m_p)}[(m_p + 1)T]}{\omega_0} &= \frac{\mathcal{E}_0 q}{M} \int_{m_p T}^{(m_p+1)T} \frac{\dot{K}[(m_p + 1)T - t_*]}{\omega_0} \sum_{m=0}^{m_p(t_*)} (-1)^m \epsilon_m \theta(t_* - mT) E'_t(t_* - mT) dt_* \\ &\quad + e^{-\Gamma_0 T} \left\{ - \left(1 + \frac{\Gamma_0^2}{\omega_0^2} \right) \sin \omega_0 T X_{(m_p)}(m_p T) + \left[\cos \omega_0 T - \frac{\Gamma_0}{\omega_0} \sin \omega_0 T \right] \frac{\dot{X}_{(m_p)}(m_p T)}{\omega_0} \right\}. \end{aligned} \quad (\text{A8})$$

As expected, the amplitude of the ladder decreases with a greater duration T of its steps, which is an obvious effect of $\Gamma_0 \neq 0$. We remind the reader that every term of the sequence $X_{(m_p)}$, $m_p = 1, 2, \dots$, implicitly bears the factor of $\mathcal{E}_0 q/M$, which initially appears in Eqs. (A3) for $m_p = 0$ and is carried through by recursion (A8).

APPENDIX B: RESONANCE FACTOR $r(\omega)$ IN TERMS OF ζ VARIABLE

In terms of the variable ζ , which is defined by the mapping (2.5), $\underline{\omega} = (\zeta + 1/\zeta)/2$, the denominator of the resonance factor $r(\omega) = [(\omega + i\Gamma_0)^2 - \omega_0^2]^{-1}$ becomes a fourth-order polynomial with respect to ζ . In what follows, $\underline{\omega}_0 = \omega_0/\Omega_e$, $\underline{\Gamma}_0 = \Gamma_0/\Omega_e$, and

$$r(\zeta) = \frac{\zeta}{\Omega_e^2 \underline{\omega}_0} \left(\frac{1}{(\zeta - \zeta_1)(\zeta - \zeta_2)} - \frac{1}{(\zeta - \zeta_3)(\zeta - \zeta_4)} \right), \quad (\text{B1})$$

with the roots $\zeta_{1,2} = (\underline{\omega}_0 - i\underline{\Gamma}_0) \pm i\sqrt{1 - (\underline{\omega}_0 - i\underline{\Gamma}_0)^2}$ and $\zeta_{3,4} = -(\underline{\omega}_0 + i\underline{\Gamma}_0) \pm i\sqrt{1 - (\underline{\omega}_0 + i\underline{\Gamma}_0)^2}$. Since the function (5.5) has no poles in the ω plane and the radius of the contour C_ζ can be made arbitrary small, it is possible to expand the resonance factor $r(\zeta)$ in ascending powers of small ζ . The algebra can be greatly simplified with an introduction of a complex angle $\vartheta = \vartheta' + i\vartheta''$ such that $\underline{\omega}_0 - i\underline{\Gamma}_0 = \cos \vartheta$, $\sqrt{1 - (\underline{\omega}_0 - i\underline{\Gamma}_0)^2} = \sin \vartheta$, and hence $\zeta_1 = e^{i\vartheta} = e^{i\vartheta' - \vartheta''}$, $\zeta_2 = 1/\zeta_1$, $\zeta_3 = -\zeta_1^* = -e^{-i\vartheta}$, and $\zeta_4 = -\zeta_2^* = 1/\zeta_3$. Then Eq. (B1) can be rewritten as

$$\begin{aligned} \Omega_e^2 \underline{\omega}_0 r(\zeta) &= \frac{\zeta}{(1 - \zeta e^{i\vartheta})(1 - \zeta e^{-i\vartheta})} - \frac{\zeta}{(1 + \zeta e^{i\vartheta^*})(1 + \zeta e^{-i\vartheta^*})} = \sum_{k=2}^{\infty} \left[\frac{\sin k\vartheta}{\sin \vartheta} + (-1)^k \frac{\sin k\vartheta^*}{\sin \vartheta^*} \right] \zeta^k \\ &= \sum_{l=1}^{\infty} \left[2 \operatorname{Re} \left(\frac{\sin 2l\vartheta}{\sin \vartheta} \right) \zeta^{2l} + 2i \operatorname{Im} \left(\frac{\sin(2l+1)\vartheta}{\sin \vartheta} \right) \zeta^{2l+1} \right], \end{aligned} \quad (\text{B2})$$

where we have noticed that the terms with $k = 0$ and $k = 1$ or, equivalently, with $l = 0$ are zero. The Taylor series for the $r(\zeta)$ begins with the term proportional to ζ^2 .

APPENDIX C: CALCULATION OF SOME INTEGRALS

The double integral (5.10) for \mathcal{E}_a is symmetric with respect to the interchange $\omega \leftrightarrow \nu$. It is sufficient to consider only one of the two terms in the numerator,

$$\begin{aligned} \frac{d\mathcal{E}_a(\tau, z < 0)}{d(\Omega_e \tilde{z}_0)} &= \frac{2\Omega_e^2 \mathcal{E}_0}{2\pi i \Omega_e} \sum_{m=0}^{m_p} \epsilon_m (-1)^m \left(\frac{-i}{4\pi} \right) \oint_{C_\omega^-} \frac{d\omega}{\omega} \mathfrak{T}[n_e(\omega)] e^{-i[\omega - \omega n_e(\omega)]\tilde{z}_0} e^{-i\omega(\tau - |\tilde{z}| - 2\tilde{z}_0 - mT)} \\ &\quad \times \oint_{C_\nu^-} \frac{d\nu}{\nu} \mathfrak{T}[n_e(\nu)] \frac{e^{-i[\nu - \nu n_e(\nu)]\tilde{z}_0}}{\nu - \omega}. \end{aligned} \quad (\text{C1})$$

The double integrals (5.11) encountered for \mathcal{E}_b , differ slightly,

$$I_1 = \oint_{C_\omega^-} \frac{d\omega}{\omega} \mathfrak{T}[n_e(\omega)] r(\omega) [2i\Gamma_0 \omega - \omega_m^2] e^{-i[\omega - \omega n_e(\omega)]\tilde{z}_0} e^{-i\omega(\tau - |\tilde{z}| - 2\tilde{z}_0 - mT)} \oint_{C_\nu^-} \frac{d\nu}{\nu} \mathfrak{T}[n_e(\nu)] \frac{e^{-i[\nu - \nu n_e(\nu)]\tilde{z}_0}}{\nu - \omega}, \quad (\text{C2})$$

$$I_2 = \oint_{C_\nu^-} \frac{d\nu}{\nu} \mathfrak{T}[n_e(\nu)] e^{-i[\nu - \nu n_e(\nu)]\tilde{z}_0} e^{-i\nu(\tau - |\tilde{z}| - 2\tilde{z}_0 - mT)} \oint_{C_\omega^-} \frac{d\omega}{\omega} \mathfrak{T}[n_e(\omega)] r(\omega) [2i\Gamma_0 \omega - \omega_m^2] \frac{e^{-i[\omega - \omega n_e(\omega)]\tilde{z}_0}}{\nu - \omega}. \quad (\text{C3})$$

We use the transformation (2.5) to trade ν in Eqs. (C1) and (C2) for a new variable ζ . This leads to the integral over a circle of an arbitrary small radius around the origin,

$$\oint_{C_\nu^-} \frac{d\nu}{\nu} \Im[n_e(\nu)] \frac{e^{-i[\nu - \nu n_e(\nu)]\tilde{z}_0}}{\nu - \omega} \rightarrow \oint^{(0+)} d\zeta \frac{1 - \zeta^2}{\zeta^2 - 2\omega\zeta + 1} e^{-i\Omega_e \tilde{z}_0 \zeta} = 0. \quad (\text{C4})$$

This integral equals zero just because its integrand is a regular function inside the contour of integration.

The integral in (C3) differs from those in (C1) and (C2) by an additional factor $r(\omega)[2i\Gamma_0\omega - \omega_m^2]$ in the integrand. According to (B2), the Taylor expansion of the resonant factor $r(\omega)$ (in terms of variable ζ) begins with ζ^2 , while $\omega \sim \zeta + \zeta^{-1}$, so the Taylor expansion of the extra factor begins with ζ^1 . Hence, this integral is also zero.

Integration (5.14) is straightforward. Multiplying the result by external factor $e^{-i\nu(\tau - |\tilde{z}|)} e^{i[\nu + \nu n_e(\nu)]\tilde{z}_0}$ from Eq. (5.13), we obtain

$$e^{-i[\nu - \nu n_e(\nu)]\tilde{z}_0} \left[(C_1 - iC_2) \frac{e^{i(\omega_0 + i\Gamma_0)\tau_*} - e^{-i\nu\tau_*}}{i(\nu + \omega_0 + i\Gamma_0)} + (C_1 + iC_2) \frac{e^{i(-\omega_0 + i\Gamma_0)\tau_*} - e^{-i\nu\tau_*}}{i(\nu - \omega_0 + i\Gamma_0)} \right], \quad (\text{C5})$$

where $\tau_* = t_{\max}^* - t_{\min}^* = \tau - |\tilde{z}| - 2\tilde{z}_0 - m_p T$ is the full time of radiation. This function has no poles in the complex ν plane.

APPENDIX D: SOURCE FUNCTIONS

The results of calculations of Sec. VI are expressed via four functions $s_j(\lambda, \xi)$, $j = 1, 2, 3, 4$. The functions $s_j(\lambda, \xi)$ are defined as the sums of the series

$$\begin{aligned} s_1(\lambda, \xi) &= \sum_{l=1}^{\infty} (-1)^l \text{Re} \left[\frac{\sin 2l\vartheta}{\sin \vartheta} \right] [\xi^{2l} J_{2l}(\Omega_e \lambda) + \xi^{2l+2} J_{2l+2}(\Omega_e \lambda)], \\ s_2(\lambda, \xi) &= \sum_{l=1}^{\infty} (-1)^l \text{Re} \left[\frac{\sin 2l\vartheta}{\sin \vartheta} \right] [\xi^{2l-1} J_{2l-1}(\Omega_e \lambda) - \xi^{2l+3} J_{2l+3}(\Omega_e \lambda)], \\ s_3(\lambda, \xi) &= \sum_{l=1}^{\infty} (-1)^l \text{Im} \left[\frac{\sin(2l+1)\vartheta}{\sin \vartheta} \right] [\xi^{2l+1} J_{2l+1}(\Omega_e \lambda) + \xi^{2l+3} J_{2l+3}(\Omega_e \lambda)], \\ s_4(\lambda, \xi) &= \sum_{l=1}^{\infty} (-1)^l \text{Im} \left[\frac{\sin(2l+1)\vartheta}{\sin \vartheta} \right] [\xi^{2l} J_{2l}(\Omega_e \lambda) - \xi^{2l+4} J_{2l+4}(\Omega_e \lambda)]. \end{aligned} \quad (\text{D1})$$

These sums are intimately connected with the Lommel functions $U_\nu(w, z)$ of two variables [24]

$$W_\nu(w, z) = \sum_{l=0}^{\infty} w^{2l} J_{2l+\nu}(z) \equiv (iw)^{-\nu} U_\nu(iwz, z). \quad (\text{D2})$$

Consider the calculation of s_1 as an example. Trading the original ϑ for $\pi/2 + \delta$ (so that $\sin \delta = -\omega_0 + i\Gamma_0$) and exercising simple algebra, we arrive at

$$\begin{aligned} s_1(\lambda, \xi) &= \sum_{l=1}^{\infty} \text{Re} \left[\frac{\sin 2l\delta}{\cos \delta} \right] [\xi^{2l} J_{2l} + \xi^{2l+2} J_{2l+2}] = \sum_{l'=0}^{\infty} \text{Re} \left[\frac{\sin(2l'+2)\delta + \sin 2l'\delta}{\cos \delta} \right] \xi^{2l'+2} J_{2l'+2} \\ &= 2\xi^2 \text{Re} \left[\sum_{l'=0}^{\infty} \sin[(2l'+1)\delta] \xi^{2l'} J_{2l'+2} \right] = 2\xi^2 \text{Re} \left\{ \frac{1}{2i} \sum_{l'=0}^{\infty} [e^{i\delta} (e^{i\delta} \xi)^{2l'} - e^{-i\delta} (e^{-i\delta} \xi)^{2l'}] J_{2l'+2} \right\}, \end{aligned} \quad (\text{D3})$$

where the argument $\Omega_e \lambda$ of the Bessel functions is omitted. Finally, referring to Eq. (D2),

$$s_1(\lambda, \xi) = -\xi^2 \text{Re} \{ i [e^{i\delta} W_2(e^{i\delta} \xi, \lambda) - e^{-i\delta} W_2(e^{-i\delta} \xi, \lambda)] \}. \quad (\text{D4})$$

In the same way, rearranging the first sum in s_2 as $l \rightarrow l' + 1$ and the second sum as $l \rightarrow l' - 1$ and subtracting the extra terms yields

$$s_2(\lambda, \xi) = 2\omega_0 \xi J_1(\Omega_e \lambda) + 4 \text{Re} \left[\sin \delta \sum_{l'=0}^{\infty} \cos(2l'\delta) \xi^{2l'+1} J_{2l'+1} \right], \quad (\text{D5})$$

which can be written as

$$s_2(\lambda, \xi) = +2\omega_0 \xi J_1(\Omega_e \lambda) + 2\xi \text{Re} \{ \sin \delta [W_1(e^{i\delta} \xi, \lambda) + W_1(e^{-i\delta} \xi, \lambda)] \}. \quad (\text{D6})$$

The two remaining functions $s_3(\lambda, \xi)$ and $s_4(\lambda, \xi)$ are transformed into

$$s_3(\lambda, \xi) = 2 \sum_{l'=1}^{\infty} (-1)^{l'} \text{Im}(\cos 2l' \vartheta) \xi^{2l'+1} J_{2l'+1} = 2\xi \sum_{l'=0}^{\infty} \text{Im}(\cos 2l' \delta) \xi^{2l'} J_{2l'+1} = \xi \text{Im}[W_1(e^{i\delta} \xi, \lambda) + W_1(e^{-i\delta} \xi, \lambda)] \quad (\text{D7})$$

and

$$s_4(\lambda, \xi) = -4 \text{Im} \left[\cos \vartheta \sum_{l'=0}^{\infty} (-1)^{l'} [\cos(2l' + 1) \vartheta] \xi^{2l'+2} J_{2l'+2} \right] = -4\xi^2 \text{Im} \left[\sin \delta \sum_{l'=0}^{\infty} \sin[(2l' + 1)\delta] \xi^{2l'} J_{2l'+2} \right] \\ = 2\xi^2 \text{Im} \{ i \sin \delta [e^{i\delta} W_2(e^{i\delta} \xi, \lambda) - e^{-i\delta} W_2(e^{-i\delta} \xi, \lambda)] \}. \quad (\text{D8})$$

The functions $s_j(\Lambda, \Xi)$ appear in Eq. (5.19) for the backward dipole radiation with the arguments $\Lambda^2 = \Omega_e^2[(\tau - |\tilde{z}| - \tilde{z}_0 - m_p T)^2 - \tilde{z}_0^2]$, $\Xi^2 = (\tau - |\tilde{z}| - 2\tilde{z}_0 - m_p T)/(\tau - |\tilde{z}| - m_p T)$, and $\Lambda \Xi = \Omega_e(\tau - |\tilde{z}| - 2\tilde{z}_0 - m_p T)$. In this study, the computational problems are somewhat alleviated by the fact that we are interested in the functions $s_j(\Lambda, \Xi)$ only at relatively small values of $\Lambda \Xi$.

The Lommel functions of two variables, despite being named long ago, have not been studied as exhaustively as, e.g., Bessel functions and there are no tables (at least for the complex-valued variables) that could have been used for the numerical calculations. *A priori*, two practical methods seem obvious. One is to cut off the number of terms in the series (D2). Another one is to use the integral representation for the Lommel functions [see Sec. 16.53(1) in Ref. [24]]

$$W_\nu(\xi, \lambda) = \sum_{l=0}^{\infty} \xi^{2l} J_{2l+\nu}(\Omega_e \lambda) = \Omega_e \lambda \int_0^1 J_{\nu-1}(\Omega_e \lambda y) \cosh \left[\frac{\Omega_e \lambda \xi}{2} (1-y^2) \right] y^\nu dy, \quad \text{Re}(\nu) > 0. \quad (\text{D9})$$

In application to our problem, the major challenge in computing these functions stems from the fact that the Langmuir frequency Ω_e is very high ($\Omega_e/2\pi \sim 10^{15}$ Hz), so the Bessel functions rapidly oscillate. Furthermore, in the integrand of (D9), the amplitude of these oscillations grows exponentially when $y \rightarrow 0$. Therefore, it is difficult to estimate the accuracy of the possible approximations. Here we attempt to combine these methods. It is straightforward to check the recursion formula

$$W_\nu(\xi, \lambda) = J_\nu(\Omega_e \lambda) + \xi^2 W_{\nu+2}(\xi, \lambda). \quad (\text{D10})$$

By iterating the recursion formula (D10) N times and applying (D9) to the $(N+1)$ st term, one readily obtains

$$W_\nu(\xi, \lambda) = \sum_{l=0}^{N-1} \xi^{2l} J_{2l+\nu}(\Omega_e \lambda) + \xi^{2N} \Omega_e \lambda \int_0^1 J_{\nu+2N-1}(\Omega_e \lambda y) \cosh \left[\frac{\Omega_e \lambda \xi}{2} (1-y^2) \right] y^{2N+\nu} dy. \quad (\text{D11})$$

When N is sufficiently large, the exponential growth of the hyperbolic cosine at $y \rightarrow 0$ and rapid oscillations of the Bessel function at $y \rightarrow 1$ in the integrand of $W_{\nu+2N}$ given by (D9) become suppressed.

In order to estimate an optimal value of the separation parameter N , we note that the lowest zero j_μ of the $J_\mu(z)$ and the first maximum j'_μ of the $J'_\mu(z)$ are greater than μ [see [24], Sec. 15.3(1)],

$$j_\mu > \mu, \quad j'_\mu > \mu.$$

For functions of large order, simple estimates of the smallest zero and the smallest maximum are (see [24], Sec. 15.83)

$$j_\mu = \mu + 1.855757\mu^{1/3} + O(\mu^{-1/3}), \quad j'_\mu = \mu + 0.808618\mu^{1/3} + O(\mu^{-1/3}). \quad (\text{D12})$$

In order that there are no zeros of the Bessel function within the interval of integration over y in (D11), it is necessary that the argument of the Bessel function does not exceed its smallest zero or its smallest maximum, i.e., $\Omega_e \lambda y < \Omega_e \lambda \leq j_{2N+\nu-1}$ or $\Omega_e \lambda \leq j'_{2N+\nu-1}$. Hence, the integral accommodates that part of the sum where order of the Bessel function exceeds its argument. The simplest estimate of $N = N(m, T)$ is given by the equations

$$\Omega_e \lambda \leq j_{2N+\nu-1} \sim 2N, \quad \Omega_e \lambda \leq j'_{2N+\nu-1} \sim 2N.$$

Numerical calculation show that for sufficiently large upper limit $N(T)$ of the sum over l , the integral in Eq. (D11) is small.

A few remarks regarding asymptotic behavior of the source functions, which clarify the origin of their behavior, observed in Figs. 8 and 9, which are based on numerical calculations and presented in Sec. VI A, are in order. The period of plasma oscillation is $\tau_e = 2\pi/\Omega_e \sim 5 \times 10^{-16} - 10^{-15}$ s and the corresponding unit of length is $\lambda_e = c\tau_e \sim 10^{-5} - 10^{-4}$ cm $\approx 10^3 - 10^4$ Å. By the nature of our problem, we are interested in the time interval $T_0 = 2\pi\omega_0 \sim 10^3 \tau_e$ so that $\Xi^2 = 1 - 2\tilde{z}_0/\tau_m$ is very close to the constant value of 1, while $\Lambda \approx \tau_m = \tau - |\tilde{z}| - m_p T$. Let us consider the limit of $\Xi = 1$ as the zeroth-order approximation when $\tau_m \gg z_0$. Curiously enough, it coincides with the exact solution with $z_0 = 0$, which corresponds to the location of the radiating dipole on the interface between vacuum and a medium. Then the functions $W_\nu(e^{i\delta}, \Lambda)$, for which, according to (D2), $(ie^{i\delta})^\nu W_\nu(e^{i\delta}, \Lambda) = U_\nu(ie^{i\delta} \Lambda, \Lambda)$, are the Lommel functions $y = U_\nu(c\Lambda, \Lambda)$ of two variables with $w = c\Lambda$, where c is constant. In our case, $c = ie^{i\delta}$, so $(c + c^{-1})^2 = 4 \sin^2 \delta$ and $y = (ie^{i\delta})^\nu W_\nu(e^{i\delta}, \Lambda)$. These functions are particular integrals of the equation

for $y = U_v(c\Lambda, \Lambda)$ [see [24], Sec. 16.52(7)]. The function $W_v(e^{i\delta}, \Lambda)$ satisfies the equation

$$4\{d^2W_v(e^{i\delta}, \Lambda)/d\Lambda^2 + \sin^2 \delta W_v(e^{i\delta}, \Lambda)\} = J_{v-2}(\Omega_e \Lambda) - e^{-2i\delta} J_v(\Omega_e \Lambda), \quad (\text{D13})$$

which obviously has, among others, the periodic solutions like $\cos(\Omega_e \Lambda \sin \delta) = \cos(\omega_0 \Lambda)$.

When $\tau \gg z_0$ it is instructive to present the functions $s_j(\Lambda, 1)$ in a somewhat different form

$$\begin{aligned} s_1(\Lambda, 1) &= 2 \operatorname{Re} \left\{ \sum_{l'=0}^{\infty} \sin[(2l'+1)\delta] J_{2l'+2}(\Omega_e \Lambda) \right\} = 2 \operatorname{Re} \left\{ \sum_{l'=1}^{\infty} \sin[(2l'-1)\delta] J_{2l'}(\Omega_e \Lambda) \right\} \\ &= 2 \operatorname{Re} \left\{ -\sin \delta \sum_{l=1}^{\infty} \cos 2l\delta J_{2l}(\Omega_e \Lambda) + \cos \delta \sum_{l=0}^{\infty} \sin[(2l+2)\delta] J_{2l+2}(\Omega_e \Lambda) \right\}. \end{aligned} \quad (\text{D14})$$

The first sum in this equation is well known to be $2 \sum_{l=1}^{\infty} \cos 2l\delta J_{2l}(\Omega_e \Lambda) = \cos(\Omega_e \Lambda \sin \delta) - J_0(\Omega_e \Lambda)$, while the second sum differs from the original one by the replacement $\sin[(2l+1)\delta] \rightarrow \sin[(2l+2)\delta]$. The function $s_1(\Lambda, 1)$ can be cast as

$$s_1(\Lambda, 1) = \operatorname{Re}\{\sin \delta [J_0(\Omega_e \Lambda) - \cos(\Omega_e \Lambda \sin \delta)]\} - \operatorname{Re}\{i \cos \delta [e^{2i\delta} W_2(e^{i\delta}, \Lambda) - e^{-2i\delta} W_2(e^{-i\delta}, \Lambda)]\}, \quad (\text{D15})$$

where $\Lambda \approx \tau_m$ and $\Omega_e \sin \delta \approx \omega_0$. In agreement with numerical calculations, the source function $s_1(\Lambda, 1)$ contains an observed sum of a slow harmonic and a precursor of the dipole radiation.

In the same way, since in Eq. (D5) $\cos 2l\delta = \cos \delta \cos(2l+1)\delta + \sin \delta \sin(2l+1)\delta$, the source function $s_2(\Lambda, 1)$ can be written as

$$\begin{aligned} s_2(\Lambda, 1) &= 2\omega_0 J_1(\Omega_e \Lambda) + \operatorname{Re} \left\{ 4 \sin^2 \delta \sum_{l=0}^{\infty} \sin[(2l+1)\delta] J_{2l+1}(\Omega_e \Lambda) + 2 \sin 2\delta \sum_{l=0}^{\infty} \cos[(2l+1)\delta] J_{2l+1}(\Omega_e \Lambda) \right\} \\ &= -2\omega_0 J_1(\Omega_e \Lambda) + 2 \operatorname{Re}\{\sin^2 \delta \sin(\Omega_e \Lambda \sin \delta)\} + 2 \operatorname{Re}\{\sin 2\delta [e^{i\delta} W_1(e^{i\delta}, \Lambda) + e^{-i\delta} W_1(e^{-i\delta}, \Lambda)]\}, \end{aligned} \quad (\text{D16})$$

where we employed another well-known result $2 \sum_{l=0}^{\infty} \sin[(2l+1)\delta] J_{2l+1}(\Omega_e \Lambda) = \sin(\Omega_e \Lambda \sin \delta) \approx \sin(\omega_0 \Lambda)$.

Using the same transformations, it is straightforward to obtain

$$\begin{aligned} s_3(\Lambda, 1) &= 2 \sum_{l=0}^{\infty} \operatorname{Im}(\cos 2l\delta) J_{2l+1}(\Omega_e \Lambda) = 2 \operatorname{Im} \left\{ \sum_{l=0}^{\infty} [\cos \delta \cos(2l+1)\delta + \sin \delta \sin(2l+1)\delta] J_{2l+1}(\Omega_e \Lambda) \right\} \\ &= \operatorname{Im}\{\sin \delta \sin(\Omega_e \Lambda \sin \delta)\} + \operatorname{Im}\{\cos \delta [e^{i\delta} W_1(e^{i\delta}, \Lambda) + e^{-i\delta} W_1(e^{-i\delta}, \Lambda)]\} \end{aligned} \quad (\text{D17})$$

and

$$\begin{aligned} s_4(\Lambda, 1) &= -4 \operatorname{Im} \left\{ \sin \delta \sum_{l'=0}^{\infty} \sin[(2l'+1)\delta] J_{2l'+2}(\Omega_e \Lambda) \right\} = 4 \operatorname{Im} \left\{ \sin \delta \sum_{l=0}^{\infty} [\sin \delta \cos 2l\delta - \cos \delta \sin 2l\delta] J_{2l}(\Omega_e \Lambda) \right\} \\ &= 2 \operatorname{Im}\{\sin^2 \delta [\cos(\Omega_e \Lambda \sin \delta) - J_0(\Omega_e \Lambda)]\} + 2 \operatorname{Im}\{i \sin 2\delta [e^{2i\delta} W_2(e^{i\delta}, \Lambda) - e^{-2i\delta} W_2(e^{-i\delta}, \Lambda)]\}. \end{aligned} \quad (\text{D18})$$

-
- [1] A. Sommerfeld, *Ann. Phys. (Leipzig)* **44**, 177 (1914).
[2] L. Brillouin, *Ann. Phys. (Leipzig)* **44**, 203 (1914).
[3] B. Macke and B. Ségard, *Eur. Phys. J. D* **23**, 125 (2003).
[4] B. Macke and B. Ségard, *Phys. Rev. A* **86**, 013837 (2012).
[5] B. Macke and B. Ségard, *Phys. Rev. A* **87**, 043830 (2013).
[6] B. Macke and B. Ségard, *Phys. Rev. A* **94**, 043801 (2016).
[7] B. Macke and B. Ségard, *Phys. Rev. A* **97**, 063830 (2018).
[8] H. Jeong, A. M. C. Dawes, and D. J. Gauthier, *Phys. Rev. Lett.* **96**, 143901 (2006).
[9] K. E. Oughstun, H. Jeong, D. J. Gauthier, and N. A. Cartwright, *J. Opt. Soc. Am. B* **27**, 1664 (2010).
[10] H. Jeong, C.-W. Lee, A. M. C. Dawes, and D. J. Gauthier, *J. Opt. Soc. Am. B* **36**, 3282 (2019).
[11] D. R. Solli, C. F. McCormick, C. Ropers, J. J. Morehead, R. Y. Chiao, and J. M. Hickmann, *Phys. Rev. Lett.* **91**, 143906 (2003).
[12] N. Brunner, V. Scarani, M. Wegmüller, M. Legré, and N. Gisin, *Phys. Rev. Lett.* **93**, 203902 (2004).
[13] L. Nanda, H. Wanare, and S. A. Ramakrishna, *Phys. Rev. A* **79**, 041806(R) (2009).
[14] K. E. Oughstun, *Electromagnetic and Optical Pulse Propagation*, Springer Series in Optical Sciences Vol. 224 (Springer, Cham, 2019), Vol. 1.
[15] K. E. Oughstun, *Temporal Pulse Dynamics in Dispersive Attenuative Media*, Springer Series in Optical Sciences Vol. 225 (Springer, Cham, 2019), Vol. 2.
[16] E. G. Skrotskaya, A. N. Makhlin, V. A. Kashin, and G. V. Skrotsky, *Sov. Phys. JETP* **29**, 123 (1969).
[17] M. Born and E. Wolf, *Principles of Optics* (Pergamon, London, 1959).
[18] L. Rosenfeld, *Theory of Electrons* (North-Holland, Amsterdam, 1951).

- [19] N. G. Denisov, *Zh. Eksp. Teor. Fiz.* **21**, 1354 (1951).
- [20] A. Sommerfeld, *Optics* (Academic, New York, 1954).
- [21] L. Brillouin, *Wave Propagation and Group Velocity* (Academic, New York, 1960).
- [22] I. N. Onishchenko, D. Y. Sidorenko, and G. V. Sotnikov, *Phys. Rev. E* **65**, 066501 (2002).
- [23] W. R. LeFev, S. Venakides, and D. J. Gauthier, *Phys. Rev. A* **79**, 063842 (2009).
- [24] G. N. Watson, *A Treatise on the Theory of Bessel Functions* (Cambridge University Press, Cambridge, 1995).
- [25] B. M. Bolotovskiy and S. N. Stoljarov, in *Problems of Theoretical Physics: A Memorial Volume to I. E. Tamm*, edited by V. Ginzburg *et al.* (Nauka, Moscow, 2008), p. 267.
- [26] A. J. Fairbanks, A. M. Darr, and A. L. Garner, *IEEE Access* **8**, 148606 (2020).
- [27] M. J. W. Rodwell, S. T. Allen, R. Y. Yu, M. G. Case, U. Bhattacharya, M. Reddy, E. Carman, M. Kamegawa, Y. Konishi, J. Pustl, and R. Pallela, *Proc. IEEE* **82**, 1037 (1994).